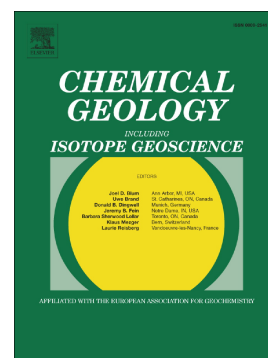


Hydrogeochemistry of trace and rare earth elements in the Caviahue-Copahue Volcanic Complex

Llano Joaquin, Calabrese Sergio, Lamberti M. Clara, Li Vigni Lorenza, Brugnone Filippo, Sierra Daniel, García Sebastián, Carbajal Fabricio, Brusca Lorenzo, D'. Alessandro Walter, Augusto Mariano



PII: S0009-2541(23)00302-9

DOI: <https://doi.org/10.1016/j.chemgeo.2023.121602>

Reference: CHEMGE 121602

To appear in: *Chemical Geology*

Received date: 10 November 2022

Revised date: 6 June 2023

Accepted date: 14 June 2023

Please cite this article as: L. Joaquin, C. Sergio, L.M. Clara, et al., Hydrogeochemistry of trace and rare earth elements in the Caviahue-Copahue Volcanic Complex, *Chemical Geology* (2023), <https://doi.org/10.1016/j.chemgeo.2023.121602>

This is a PDF file of an article that has undergone enhancements after acceptance, such as the addition of a cover page and metadata, and formatting for readability, but it is not yet the definitive version of record. This version will undergo additional copyediting, typesetting and review before it is published in its final form, but we are providing this version to give early visibility of the article. Please note that, during the production process, errors may be discovered which could affect the content, and all legal disclaimers that apply to the journal pertain.

Volcanic Complex

Llano Joaquín^{1,2,*}, Calabrese Sergio^{3,4}, Lamberti M. Clara^{1,2}, Li Vigni Lorenza⁴, Brugnone Filippo⁴, Sierra Daniel^{2,5}, García Sebastián⁶, Carbajal Fabricio⁶, Brusca Lorenzo³, D'Alessandro Walter³, Augusto Mariano^{1,2}

¹ Universidad de Buenos Aires, Facultad de Ciencias Exactas y Naturales, Departamento de Geología, Grupo de Estudio y Seguimiento de Volcanes Activos (GESVA), Buenos Aires, Argentina.

² Instituto de Estudios Andinos “Don Pablo Groeber” (IEA/N), Universidad de Buenos Aires – CONICET, Buenos Aires, Argentina.

³ Istituto Nazionale di Geofisica e Vulcanologia - Sezione di Palermo, Palermo, Italia.

⁴ Dipartimento di Scienze della Terra e del Mare - DiSTeM, Università di Palermo, Palermo, Italia.

⁵ Instituto Geofísico de la Escuela Politécnica Nacional, Quito, Ecuador

⁶ Observatorio Argentino de Vigilancia Volcánica (OAVV), Servicio Geológico Minero Argentino (SEGEMAR), Buenos Aires, Argentina.

* Corresponding author at: Intendente Güiraldes 2160, CABA, Argentina.

Email address: jllano@gl.fcen.uba.ar (J. Llano).

The Caviahue-Copahue Volcanic Complex is one of the most studied active volcanic systems in the South American Andean range, and yet little research has focused on trace and rare-earth elements of waters, especially during an eruptive cycle. In this study, we sampled and investigated natural waters from 23 sites (involving the crater lake, hot springs, streams, rivers, and bubbling pools) in two campaigns in 2017 and 2018, using physicochemical parameters, major, trace and rare-earth elements concentrations. With this novel dataset, it was possible to identify, characterize and compare three groups of waters with distinctive hydrofacies. Indeed, the normalization of water compositions against host rock concentrations showed a particular trace element pattern for each group of waters. Although the absolute concentrations of the elements in each sampling site changed from 2017 to 2018, the normalized patterns did not. Boron, As, Cd, Tl, Se, and Te, commonly recognized as volatile, are the main trace elements that magmatic gases supply to the system headwaters, whereas elements such as Ca, K, and Ba are affected by precipitation of secondary minerals (gypsum, anhydrite, barite, jarosite, and alunite). Furthermore, the main river draining the summit volcano shows a steady decrease in As, Cr, and V concentrations correlated to the precipitation of Fe and Al hydroxysulfates (schwertmannite and basaluminite, respectively). Moreover, it is the first time that a comparison between the different water groups is made using the patterns of the rare-earth elements, allowing us to identify and separate depletion patterns due to dilution processes from those due to precipitation processes.

Keywords: Copahue volcano; Hydrological system; Geothermal; Trace elements; Rare-earth elements

1. Introduction

Many volcanoes show important associated hydrological systems (e.g. Giggelbach, 1992; Rowe, 1994; Kusakabe et al., 2000; Varekamp, 2015; Benavente et al., 2016; Tassi et al., 2016; Romero-Mujalli et al., 2022). Studying the interaction between magmatic gases, host rocks, and hydrothermal aquifers is crucial for a better understanding of the whole volcanic system, as well as for monitoring volcanic activity (e.g. Taran et al., 2008; Agosto et al., 2012; Varekamp, 2015; Rouwet et al., 2017). Numerous studies in other volcanoes of the world have characterized the volcanic system using geochemical analyses with particular emphasis on the hydrological system (e.g. Deely and Sheppard, 1996; Delmelle et al., 2000; D'Alessandro et al., 2004; Palmer et al., 2011; Liotta et al., 2016; Rouwet et al., 2017).

The most distinctive geographical feature of the Caviabue-Copahue Volcanic Complex (CCVC) is Copahue volcano ($37^{\circ}51'08''\text{S}$ - $71^{\circ}10'03''\text{W}$). The frequent explosive activity, the proximity of two important tourist localities to the active crater (Copahue and Caviabue, ~6 and 9 km, respectively), and the promising geothermal prospect of this hydrothermal system has aroused great interest among the scientific community over the last three decades (e.g. Delpino and Bermudez, 1993; Mas et al., 1996; Panarello, 2002; Naranjo and Polanco, 2004; Parker et al., 2008; Agosto et al., 2013; Caselli et al., 2016; Agosto and Velez, 2017; Roulleau et al., 2016; Daga et al., 2017; Tassi et al., 2017; Barcelona et al., 2019; Lamberti et al., 2019; Bia et al., 2020; Candela-Becerra et al., 2020).

The acid gases that are constantly emitted from the deep magmatic chamber (about 5 km depth; Velez et al., 2011) interact and acidify the waters of the system, both in the shallow brine within the volcano and in the deep aquifer related to the geothermal reservoir (Agosto et al., 2012; Agosto et al., 2013; Barcelona et al., 2019). Although extensive research has been carried out on the CCVC water geochemistry, most studies have only focused on major ions, not treating minor and trace elements in much detail (Varekamp et al., 2009; Farnfield et al., 2012; Alexander, 2014; Tardani et al., 2021), except for Gammons et al. (2005), Parker et al. (2008) and Llano et al. (2021) where a good description of some trace elements along the Agrio river is made.

The main aim of this study is to investigate the processes controlling the chemical characteristics of the different water groups using 32 minor and trace elements. Thirty-seven samples were collected

in the summer of 2017 and 2018 where we analysed minor and trace elements from samples taken in both years and rare earth elements from the 2018 samples. The results of these analyses allowed to make inferences about the chemical processes acting in the CCVC hydrological system throughout the current eruptive cycle, with special emphasis in the volatile trace elements (As, Tl, Se, Cd, B, Pb, and Bi; Aiuppa et al., 2000a; Calabrese et al., 2011; Scholtysic and Canil, 2018; Inostroza et al., 2023), which can be enriched in waters affected by magmatic gases and aerosols. Therefore, we present data of these elements in the CCVC headwaters and geothermal field waters, in order to identify which of them are incorporated to the hydrological system. So doing it, we add a new piece in the puzzle of CCVC, linking the changes in surface waters composition to the activity within the deep magmatic-geothermal system. Such data may also be an important tool for volcanic surveillance.

2. Geological setting

2.1 Geology

The study area is located in the central segment of the South Volcanic Zone (latitude 33° S - 46° S; Cembrano and Lara, 2009). Copahue volcano (Fig. 1) is an active andesitic to basaltic stratovolcano that first erupted at 1.2 Ma (Linares et al., 1999), and it is located on the western border of the Agrio caldera, which is part of the CCVC. The basement rocks of the area are volcanic breccias and basaltic and andesitic flows from the Cola de Zorro Formation (Linares et al., 1999; Varekamp et al., 2006; Roulleau et al., 2018). The more abundant rocks in the Agrio caldera belong to the Las Mellizas Formation, which is composed of three sequences: lower flows, ignimbrites, and upper flows (Melnick et al., 2006; Roulleau et al., 2018). The Copahue volcano activity over the last 1 Ma has generated basaltic and basaltic-andesitic flows classified as pre-, syn- and post- glacial (Muñoz and Stern, 1988; Linares et al., 1999; Roulleau et al., 2018; Albite et al., 2019; Baez et al., 2020; Sruoga et al., 2021).

The Copahue volcano presents nine craters oriented N40 E, the easternmost being the most presently active. Eruptions have been constant over the last 250 years, with phreatomagmatic and phreatic characteristics (Naranjo and Polanco, 2004). The last eruptive cycles occurred in the years 1992, 2000, and 2012 to the present (Delpino and Bermudez, 1993, 2002; Petrinovic et al., 2014; Caselli et al., 2016; Agosto and Velez, 2017; Agosto et al., 2017). This last cycle gave place to ash columns, predominantly with east and south-east directions (Daga et al., 2017; Hantusch et al., 2021; Paez et al., 2021; Bia et al., 2022). During quiescent periods, the volcano hosts a thermal hyperacid crater lake and hot springs flowing from the east flanks. The volcanic activity affects the geochemistry of some of the waters in the CCVC (Agusto and Varekamp, 2016); the pH decreases and the conductivity and major ions concentrations increase.

The CCVC hosts a geothermal field located to the northeast of the volcano (Fig. 1). This system is fed by a 800 m-depth aquifer that discharges fluids from five areas. These fluid emissions are boiling and bubbling waters, mud pools with temperatures up to 96 °C and boiling fumaroles (~90 °C at 2000 m a.s.l.; Agosto et al., 2016; Roulleau et al., 2016; Tassi et al., 2017; Tardani et al., 2021).

2.2 Hydrogeochemistry of the Cavahue-Copahue Volcanic Complex

The CCVC presents a variety of surface waters including lakes, lagoons, rivers, minor streams, ephemeral rivers, bubbling pools, and small ponds (Fig. 1). These water bodies have different geochemical characteristics and were classified by Agosto (2011) into three distinct groups: snow melt waters (MW), waters from the volcanic hydrological system (VHS), and steam heated waters (SHW).

The MW originate predominantly from snow melting and, to a lesser extent, from rainwater, with typical meteoric compositions, neutral pH, and low electrical conductivity (EC) values (20 - 800 $\mu\text{S}/\text{cm}$).

The VHS comprises the waters draining from the volcano summit. From the headwaters, this group is fed by waters with very low pH (0.1 - 2) and high EC (1,000 – 65,000 $\mu\text{S}/\text{cm}$). The high

Concentrations of cations and anions are controlled by the interaction among meteoric water, magmatic gases, and host rocks. The acid magmatic gases (CO_2 , SO_2 , HCl , HF) interact with the aquifer and enrich the water with major anions (SO_4^{2-} , Cl^- , F^-) by solubilization and dissociation reactions. Due to the strong acidity of the water, CO_2 does not form HCO_3^- (Agusto and Varekamp, 2016). The major cations (Na , K , Ca , Mg), minor cations (Fe , Al), and trace elements are readily released from the host rock to the solution. This process is favored by the low pH and the high temperatures (30 to 70 °C) of the waters. VHS waters are therefore strongly influenced by volcanic activity.

SHW are located in the geothermal field near Copahue village (Fig. 1). Here, different from the crater, a deep aquifer scrubs most soluble magmatic gases (HCl , HF) and reduces SO_2 to H_2S (Panarello, 2002; Agusto, 2011; Barcelona et al., 2019; Tardani et al., 2021). Therefore, the SHW present acid (2 - 3.5) to neutral pH and high EC (2,000 - 7,500 $\mu\text{S}/\text{cm}$), and differ from VHS waters by presenting low F^- (<0.05 - 5 mg/L) and Cl^- (<0.61 - 4.0 mg/L) concentrations.

3. Materials and methods

3.1 Sampling sites

Two field campaigns were carried out in February and March 2017 and 2018, and surface waters were collected from 23 sites (Fig. 1), totaling 37 samples. Based on previous studies, sampling sites were selected to include waters from the three groups classified by Agusto (2011).

In 2017, the crater lake was dry (Agusto et al., 2017; Baez et al., 2020), whereas two separate small lakes were observed at the bottom of the crater in 2018 (Fig. 2a). Due to the danger of sampling the hot crater lake, we collected a sample from a cold small lake (Site 1). We also collected samples from two thermal and hyperacid springs that are discharged from the east flank. These springs are well known in the literature as *vertientes*, defined as South and North springs (Sites 2 and 3, respectively; Fig. 2b) and fed by the volcanic hyperacidic brines developed below the crater. Waters from these distinct springs merge downstream to form the upper Agrio river (Sites 4, 5, 6, 7, and 8;

Fig. 2b). This river discharges its waters into Caviahue lake (Site 9; Fig. 2b and 2c) after flowing through a 18-km-course on the eastern flank of the volcano. Caviahue lake has a horseshoe form formed by a structural graben (Melnik et al., 2006; Varekamp, 2008). The lower Agrio river (Sites 10, 11, 12, 13, and 14) is the only effluent of Caviahue lake, located in the north arm of the lake. The Agrio river, along both sections, and Caviahue lake are fed by MW (Fig. 1) from the Pucón Mahuida stream (Site 15; Fig. 2d), Dulce river, Trolope river (Site 16; Fig. 2e), Cajón Chico stream, Ñorquin river outside the caldera (Site 17), and by tributaries active only during the spring and summer. Moreover, there is a small number of lakes in the Agrio caldera: we sampled Las Mellizas lake (Site 18; Fig. 2b) as representative of these waters. We also analyzed a minor stream, Colorado stream (Site 19), which had only been described by Rodríguez et al. (2016). This minor tributary also drains waters from the eastern flank of Copahue volcano (Fig. 1) and merges with the upper Agrio river (Site 5), with acid pH and similar ionic concentrations to this river.

The SHW are located in the geothermal zone (Fig. 1). We sampled four representative waters from this group, Las Máquinas (Site 20; Fig. 2f), Las Maquinitas (Site 21; Fig. 2g), Agua del Limón (Site 22) and Anfiteatro (Site 23). The first two are acid and hot bubbling pools, with diameters of about tens of meters, whereas Agua del Limón (acid and hot), and Anfiteatro (neutral and warm), are pools of less than one meter diameter.

3.2 Field measurements, sampling methods and laboratory analysis

Physicochemical parameters (temperature, pH, and EC) were measured directly in the field by a portable multiparameter instrument HANNA HI 991301. Filtered samples (0.45 μm) were collected in 250 ml plastic bottles for anions analysis (SO_4^{2-} , HCO_3^- , Cl^- , F^-) and in 150 ml plastic bottles for cations (Na, K, Ca, Mg, Fe, Al, Si), trace, and rare-earth elements (REE); the aliquot for cations, trace elements, and REE was acidified by HNO_3 Suprapur until reaching pH below 2. In the case of thermal waters ($T > 40^\circ\text{C}$), an aliquot for Si determination was collected and diluted with Millipore water (volume ratio 1:10) to avoid precipitation of silicate minerals.

Major ions were analyzed in the laboratories of the Servicio Geológico Minero Argentino - SEGEMAR (Argentine Geological Mining Service). Anions were determined following the 4110 B

measured from the Standard Methods (23rd Edition), by using a Metrohm 850 Professional ion chromatograph equipped with a Metrosep A Supp 5 column. The detection limits (mg/L) were 0.05 for F, SO₄, and HCO₃ and 0.01 for Cl. The analytical errors were $\leq 5\%$. Cations were detected by using an ICP-OES Optima 5300 DV Perkin Elmer, following the 3120 B method from the Standard Methods (23rd Edition). The detection limits (mg/L) were 0.01 for Mg and 0.05 for K, Ca, and Na, while the analytical errors were $\leq 10\%$. Trace elements and REE were analyzed at the Istituto Nazionale di Geofisica e Vulcanologia (INGV) of Palermo (Italy), by inductively coupled plasma mass spectrometer (ICP-MS) using an Agilent 7500ce instrument, with precision always better than 3%. Calibration solutions for all investigated elements were prepared daily using an appropriate dilution of 100 mg/L and 1000 mg/L of stock standard solutions (Merck) with 0.14 mol/L high-purity nitric acid.

The quality assurance and quality control (QA/QC) procedures included: field and analytical blanks, cleaning procedures, and field and inter-laboratory comparison. In addition, some samples (one from each water group) were analyzed as duplicate to check for reproducibility, and reagent blanks were analyzed with samples to check baseline contamination. All the blanks collected in field present results below detection limit. The analytical accuracy of trace element determinations was checked by the analysis of four Certified Reference Materials (TM Rain 04, SLR4, SLRS5, SPSSW1).

The geochemical modeling program PHREEQC 3.1.4 version (Parkhurst and Appelo, 2013), with Minteq database, was used to calculate the saturation indexes for relevant solids in the VHS headwaters and the SHW.

3.3 Previous data

A comparison with the host rock geochemistry was necessary to understand the different processes that occur in the study system. Therefore, an average rock composition was chosen by using the data from Roulleau et al. (2018), which includes the main rocks from the Agrio caldera basement, Las Mellizas sequence, and flows from the major eruptive episodes of Copahue volcano. To

Compare Li, B, Br, Cd, Se, and Te, which are not available in Rouillard et al. (2018) dataset, we used an upper continental rock composition from Wedepohl (1995).

Water geochemical analyzes published in previous studies (Gammons et al., 2005; Parker et al., 2008; Chiacchiarini et al., 2010; Agosto et al., 2012; Alexander, 2014; Agosto and Varekamp, 2016; Rodriguez et al., 2016) were also used together with the new data for Figs. 6 and 7 in the discussion section. Here, Cl concentrations were used as reference as it is a conservative ion (Agosto, 2011; Agosto and Varekamp, 2016; Llano et al., 2020).

4. Results

4.1 Physicochemical parameters and major ions

The temperature, pH, conductivity, and major ions concentrations from the 2017 and 2018 samples are listed in Table 1. As previously established by the literature, the VHS headwaters and SHW are acid waters (pH ranging from 1.5 to 3.7), whereas the MW have almost neutral pH values between 5.5 and 7.5. The VHS headwaters and the SHW present high EC (2,400 - >20,000 $\mu\text{S}/\text{cm}$), although the VHS downstream show progressively decreasing EC from 900 to 150 $\mu\text{S}/\text{cm}$. The VHS headwaters present high concentrations of SO_4 (1,600 - 11,000 mg/L), Cl (500 - 6,000 mg/L) and F (30 - 180 mg/L), that decrease downstream (SO_4 : 50 - 700 mg/L; Cl: 17 - 240 mg/L; F: 0.75 - 10 mg/L). The SHW present high SO_4 concentrations (750 - 4,500 mg/L), but low Cl (<0.01 - 35 mg/L) and F (<0.01 - 2.5 mg/L). Bicarbonate is absent in both groups due to the acidity of the waters. The MW EC values are below 500 $\mu\text{S}/\text{cm}$, except for the Pucón Mahuida stream (Site 15) that has an EC of 800 $\mu\text{S}/\text{cm}$. Anion concentrations of this group of waters are variable (HCO_3 : 14 - 120 mg/L; SO_4 : 7.5 - 320 mg/L; Cl: 2 - 100 mg/L; F: 0.1 - 3 mg/L). The crater lake sampled in 2018 (Site 1) was cold (8 °C), with acidic pH (3.5) and low EC (280 $\mu\text{S}/\text{cm}$), far from the historical thermal hyperacidic values of the crater lake (Agosto and Varekamp, 2016). This crater lake represents a primary stage of the developing crater lake after the strombolian 2016-2017 eruptions

(Agusto et al., 2017; Dac2 et al., 2020), and it was only indirectly affected by the volcanic plume and not by direct fumarolic input.

In the VHS headwaters the major cations present the highest values of all samples (Na: 85 - 565 mg/L; K: 9 - 55 mg/L; Ca: 190 - 680 mg/L; Mg: 240 - 1760 mg/L; Fe: 80 - 1,050 mg/L; and Al: 85 - 720 mg/L), with decreasing concentrations downstream (Na: 7 - 95 mg/L; K: 2 - 11 mg/L; Ca: 12 - 170 mg/L; Mg: 10 - 285 mg/L; Fe: 0.03 - 90 mg/L; and Al: 0.03 - 190 mg/L). The SHW present lower values than the VHS headwaters (Na: 7 - 25 mg/L; K: 1 - 7 mg/L; Ca: 12 - 60 mg/L; Mg: 3.5 - 30 mg/L; Fe: 1 - 115 mg/L; and Al: 0.05 - 160 mg/L). Whereas the MW present very low cation concentration values (Na: 2 - 20 mg/L; K: 0.8 - 6.5 mg/L; Ca: 5 - 60 mg/L; Mg: 3 - 55 mg/L) specially for Fe (0.02 - 0.04 mg/L) and Al (0.01 - 2 mg/L).

The classification proposed by Agusto (2011) for the CCVC waters was based on the main ions composition and it has been adopted also for this work. The major ions of the 2017 and 2018 samples have been plotted in Fig. 3, together with the rock data reported by Roulleau et al. (2018). The VHS waters have SO₄-Cl composition with major cation composition that fall near the rock field but with an enrichment in Mg. The MW samples are HCO₃ to SO₄-HCO₃ dominant with a major cation composition that falls in the rock composition range. The Pucón Mahuida stream (Site 15) presents a particular case, with anionic composition more similar to the VHS, also recognized in the F concentrations (1.9 - 2.8 mg/L). The SHW are SO₄ dominated, some samples present cation compositions that fall into the rock composition field, whereas four samples show lower Mg values. The only SHW water sample that presents a distinctive composition within this group is Anfiteatro (Site 23), showing anionic composition more similar to the MW. The Colorado stream (Site 19) show a riverbed covered by a red ochre precipitate, described as iron hydroxide minerals by Rodriguez et al. (2016). This site is classified in this work as part of the VHS waters, because it shows similar values to the group with pH ranging from 3.2 to 3.8, EC of 3,310 µS/cm, and similar ionic compositions with respect to the VHS, including F (14 mg/L).

4.2 Trace elements

Table 2 shows the trace elements results of this survey. The most abundant trace elements are B, Li, Mn, Sr, and Zn, presenting values from 70 to 57,000 $\mu\text{g/L}$ for the VHS headwaters, decreasing these values (1.5 - 12,000 $\mu\text{g/L}$) downstream. In the SHW these elements present values from 3 to 4,000 $\mu\text{g/L}$, from 2 to 2,250 $\mu\text{g/L}$ in the MW, and from 160 to 40,500 $\mu\text{g/L}$ in Colorado stream. Arsenic, Ba, Be, Cd, Co, Cr, Cu, Ni, Rb, Ti, V, and Y present concentrations between 0.1 and 3,000 $\mu\text{g/L}$ in the VHS headwaters, between 0.05 and 260 $\mu\text{g/L}$ in VHS downstream, between 0.5 and 180 $\mu\text{g/L}$ in the SHW, between 0.02 and 22 $\mu\text{g/L}$ in the MW, and between 0.1 and 210 $\mu\text{g/L}$ in Colorado stream. Whereas Bi, Cs, Hf, Mo, Pb, Se, Sn, Ta, Te, Th, Tl, U, and Zr present much lower concentrations: <0.001 to 75 $\mu\text{g/L}$ in the VHS headwaters, <0.001 to 13 $\mu\text{g/L}$ in the VHS downstream, <0.001 to 6 $\mu\text{g/L}$ in the SHW, <0.001 to 2 $\mu\text{g/L}$ in the MW, and <0.001 to 5 $\mu\text{g/L}$ in Colorado stream.

The composition of one representative sample for each group of the CCVC waters (MW: Trolope river, Site 16; VHS: North spring, Site 3; SHW: Las Máquinas, Site 20) from the 2017 campaign is plotted in Fig. 4. The Trolope river represents what we define as the background composition of the area, as this sample is least affected by volcanic gases and ash emissions (Agusto, 2011; Gammons et al., 2005; Llano et al., 2020). This MW presents lower concentrations in all the species in comparison with the North spring and Las Máquinas samples.

4.3 Rare earth elements

The REE concentrations from the 2018 campaign samples are shown in Table 3. VHS headwaters present total REE concentrations from 1,540 to 1,950 $\mu\text{g/L}$, with decreasing values downstream (19 - 370 $\mu\text{g/L}$). The SHW have total REE concentrations from 24 to 200 $\mu\text{g/L}$. Among the MW, Pucón Mahuida stream has higher concentrations (67 $\mu\text{g/L}$) than the cold crater lake (11 $\mu\text{g/L}$). Colorado stream presents total REE concentrations of 205 $\mu\text{g/L}$.

Water samples REE concentrations were normalized to NASC rock samples (Gromet et al., 1984) and arbitrary subdivided in light REE (from La to Sm) and heavy REE (from Gd to Lu). The ratios $\text{La}_{\text{NASC}}/\text{Sm}_{\text{NASC}}$ and $\text{Gd}_{\text{NASC}}/\text{Lu}_{\text{NASC}}$ were used to quantify the enrichment or depletion in both REE subgroups. Whereas Eu and Ce anomalies were calculated by: $\text{REE}_n/\text{REE}_{n\text{NASC}}^* = \text{REE}_{n\text{NASC}}/(\text{REE}_n$

$IN_{ASC} = REE_n / REE_{n+1NASC}$, where REE_{nNASC} is the chosen element concentration to calculate the anomaly, while $REE_{n-1NASC}$ and $REE_{n+1NASC}$ represent the previous and the subsequent element along the REE series, respectively. Values of <0.8 are indicative of negative anomalies, whereas those >1.2 to positive anomalies (Grawunder et al., 2014; Migaszewski et al., 2016).

The VHS headwaters present La_{NASC}/Sm_{NASC} values that vary between 0.91 to 1.11, decreasing these values to 0.85 to 0.72 downstream. In the MW and Colorado stream these ratios vary from 0.51 to 0.82. Whereas in the SHW these values vary from 0.29 to 0.57. The Gd_{NASC}/Lu_{NASC} values are of 1.10 to 1.29 in the VHS headwaters, increasing these values downstream to 1.28 to 1.53. The Colorado stream have a value of 1.45 and in the MW these values are of 2.09 and 2.44. The SHW present values of 1.27 to 1.47.

Most of the samples do not present Eu anomalies (values between 0.88 to 1.20), except for the cold Crater Lake (0.75), Colorado stream (0.64), Pucón Mañada stream (0.62), and Salto del Agrio sample in the lower agrio river (0.76; site 11) that present negative anomalies. Whereas the Ce anomalies are in the range of 0.82 to 1.20 for all the samples.

5. Discussion

Cations, minor, and trace elements can be divided into four groups based on their mobility in the aqueous environment (Boes and Mesmer, 1976; Stumm and Morgan, 1996; Aiuppa et al., 2000a; Aiuppa et al., 2000b; Aiuppa et al., 2005): i) the alkaline and alkaline earth elements (Na, K, Ca, Mg, Li, Ba, Be, Cs, Rb, Sr) that are very mobile because they are largely dissolved as free ions due to their electronic configuration; ii) the mobile elements (As, Bi, Mo, Se, Tl, U) that form oxyanions because of their high hydrolyzing power in their higher oxidation state, depending on the pH and redox conditions; iii) the transition elements (Fe, Mn, Cd, Co, Cr, Cu, Ni, Pb, Sn, Te, V, Zn), including the REE, that have a lower tendency to form complexes, depending on availability and concentration of ligands; and iv) the immobile elements (Al, Hf, Ta, Th, Y, Ti, Zr), which are typically difficult to remove from the rock or tend to form secondary minerals during host rock weathering in neutral pH waters. However, acidic pH will favor solubility of immobile element.

The principal source of trace elements in natural water is water-rock interaction (Baes and Mesmer, 1976; Stumm and Morgan, 1996). Nevertheless, in volcanic environments, the contribution from volcanic gases to waters can be considerable, especially for elements like As, B, Cu, Pb, Sb, Tl, Mo, and Zn (Aiuppa et al., 2000a; Calabrese et al., 2011; Scholtysic and Canil, 2018; Inostroza et al., 2023).

The differences in physicochemical values and ion concentrations between the 2017 and 2018 samples are largely due to two main processes occurring in the system. On the one hand, the activity of Copahue volcano can vary from year to year, with fluctuating magmatic gas input. When this activity increases, it favors the formation of hotter and more acidic waters that can more effectively dissolve host rock, thereby reaching higher ionic concentrations (Agusto and Varekamp, 2016). Also, during this activity fresh magma can be injected into subsurface, or ash deposited on the surface, providing fresh rock that has not been previously leached, contributing to increase some elements concentrations after an eruption. On the other hand, meteoric recharge and the higher contributions from MW to the VHS and SE W can dilute these waters, raising the pH and reducing the temperature, EC, and ion concentrations. Both processes continually compete to determine the physicochemical characteristics and compositions of the waters. The impact of these processes on the water compositions can be visualized by normalizing to the composition of the rock (Fig. 5).

5.1 Trace element patterns

5.1.1 Melt waters (MW)

The trace elements patterns for MW/rock values are shown in Fig. 5. The Pucón Mahuida stream and the Trolope river samples (Sites 15 and 16, respectively) present almost identical patterns. Both have similar ratios for the alkaline and alkaline earth elements, except for Ba. Low ratios of Fe, U, Cr, V, Ti, Mn, and Al comparing to Na are found due to hydroxide precipitation, as observed elsewhere (Baes and Mesmer, 1976; Stumm and Morgan, 1996; Rodriguez et al., 2016). However, enrichment in Al, Mn, Y, Co, Cd, Se, and Ni comparing to Na are particularly identified only in Pucón Mahuida stream, which is related to its proximity and downwind location with respect to the

Volcanic Emission Vent (Daga et al., 2017; Llano et al., 2020; Paez et al., 2021), which is reflected also in the F concentrations of these samples (Table 1; Bia et al., 2020; Paez et al., 2021). During eruptive periods, the Pucón Mahuida stream is strongly affected by volcanic ashfall due to the predominant wind direction (NW-SE). The Pucón Mahuida pattern is similar for 2017 and 2018. On the other hand, the Ñorquin river (Site 17) is expected to present a different trace elements pattern because its basin is distant from the CCVC, to the north-east of the study area (Fig. 1). The major cations have similar ratios, whereas Be, Cs, and Rb are depleted.

5.1.2 Volcanic hydrological system (VHS)

The normalized trace elements in the VHS headwaters with respect to the rock composition are presented in Fig. 5. The hyperacidic brine in the volcanic edifice that feeds the spring waters is directly affected by magmatic gas contributions (Gammons et al., 2005; Agosto and Varekamp, 2016), providing not only higher element concentrations but also a particular fingerprint to the springs. The alkaline and earth alkaline element ratios show similar values, with a light enrichment in Mg compare to Na due to the dissolution of fresh igneous rock incorporated into the system during every active period (Varekamp et al., 2009). All the spring samples show a slight depletion in Ca comparing to Na because of gypsum and anhydrite precipitation (Gammons et al., 2005; Varekamp, 2015). Both minerals present saturation indexes (SI) near to equilibrium in these samples (from -0.58 to -0.02), and oversaturated in the South spring from 2018 (0.05 for gypsum and 0.15 for anhydrite). The lower K ratios than Na are likely related to jarosite and alunite precipitation (Varekamp et al., 2009; Varekamp, 2015; Agosto and Varekamp, 2016). Jarosite is oversaturated in all the spring samples (SI values from 3.8 to 4.3), whereas alunite is undersaturated (-6 to -1.59) in both years. An extreme depletion in Ba is also recognized, due to barite precipitation within the hydrothermal system that feeds the springs (Gammons et al., 2005); consistent with near equilibrium to oversaturated SI values (-0.12 to 0.47) for this mineral. Boron, As, Cd, Tl, Se, and Te present significantly higher ratios than Na (very mobile elements), especially in the springs samples. This is related to the strong contribution of magmatic fluids feeding the hydrothermal

waters system (Calabrese et al., 2011; Varekamp, 2015; Wraage et al., 2017). Manganese, Co, Ti, and Zn present similar ratios to Na due to their release to the waters from fresh igneous rock incorporated during active periods (Varekamp et al., 2009), especially for the spring samples of 2018. The patterns show a depletion in Ti and Zr in comparison to Na according to their low tendency of being leached from the host rock. Tin and Mo are depleted in comparison to Na, as they can precipitate as secondary minerals like cassiterite (SnO_2) or molybdenite (MoS_2) in the system (Varekamp et al., 2009), or not being liberated from the host rock. The Colorado stream pattern is similar to the spring patterns. However, Colorado stream differs from the rest of the VHS because As, Cr, and V ratios are depleted relative to Na, due to the adsorption of these elements onto the hydroxides precipitating along this stream bed (Rodriguez et al., 2016). These elements are prone to form oxyanions that are easily adsorbed onto iron oxyhydroxide minerals (Elizalde-González et al., 2001; Aiuppa et al., 2003; Naeem et al., 2007; Guan et al., 2008; Parker et al., 2008; Ajouyed et al., 2010). An identical pattern but with lower concentrations for the 2017 samples is observed. The 2018 spring samples show higher ratios for most of the elements due either to more intense magmatic gas fluxes, or to a lower meteoric recharge in the area. The second possibility is excluded, due an increase in the precipitations in the year 2017 (1,301 mm) compared to 2016 (1,021 mm) for the area (AIC, 2017; AIC, 2018). Therefore, as the samples were taken in March 2017 and March 2018, a raise in the magmatic mass and energy fluxes can be hypothesized in the year 2018 comparing to the previous one.

5.1.3 Steam heated waters (SHW)

The SHW show flatter patterns than the VHS (Fig. 5). New magma-feeding do not occur in the geothermal areas, for this reason, water-rock interaction processes are more stable than in the VHS area (Varekamp et al., 2009; Agosto, 2011; Gaviria Reyes et al., 2016). Arsenic, Tl, Se, and Te do not present enriched values compared to Na, as these elements tend to precipitate as secondary minerals in the deep aquifer, especially As as sulfides (Farnfield et al., 2012; Wraage et al., 2017). Boron and Cd present an enrichment comparing to Na for the 2017 samples, due to the input of

deep magmatic-hydrothermal vapors in the aquifer (Wrage et al., 2017). The SHW samples show depleted values in Ba due to barite precipitation (Wrage et al., 2017), as they have SI near to equilibrium for this mineral in both years (SI from -0.4 to -0.08), and oversaturated in Las Máquinas in 2017 (0.16). Titanium, Hf, and Zr can be scarcely leached from the host rock presenting depleted ratios compare to Na. Lower ratios than Na in transition elements (Co, Cr, Cu, Ni, Sn, Mn, and Mo) are recognized, possibly due to mineral precipitation or also by a low tendency of been liberated during water-rock interaction.

As seen in the VHS, the 2018 samples present higher ratios than 2017. Due to the higher amount of precipitations in the year 2016 over 2017 (AIC, 2017; AIC, 2018) an increment of deep magmatic-hydrothermal gas flux can be supposed from 2017 to 2018.

Finally, Anfiteatro sample has not been plotted in Fig. 5 due to its low concentration values for most of the trace elements. This sample was a small pond less affected by magmatic or geothermal gases.

5.2 Trace elements along the Agrio river system

To complete the study of the CCVC hydrological system, it is important to consider the behavior of trace elements along the Agrio river. Therefore, major ions (SO_4 , Na, Fe, and Al) and some trace elements (Sr, Zn, As, V, and Cr) with respect to Cl concentrations were used as representatives to analyze this behavior. Comparing the present data with those of previous authors, no significant differences were recognized, indicating a stability of the system through the years.

Sulfate, Na, Sr, and Zn were normalized by Cl concentrations (Fig. 6a) and plotted versus distance from the crater lake. Sulfate shows no significant variation in the VHS waters. The conservative behavior of this species suggests that dilution along the Agrio river system due to the MW inflow is the primary control over the decrease in concentrations (Gammons et al., 2005; Agosto et al., 2012; Llano et al., 2020) as is recognized by the +1.0 slope trend in Fig. 6b. This conservative behavior is representative of most of the elements in the VHS waters. Nevertheless, there are some elements, as Na and Sr, where an enrichment along the Agrio river can be recognized, evidenced in the Na/Cl and Sr/Cl values (Fig. 6a). The <1.0 slope trend in Fig. 6b indicates inputs of Na and Sr in the Agrio

river by the MW tributaries and groundwater with low Cl concentrations. Zinc has a conservative behavior similar to SO_4 , but a depletion can be recognized after the entrance of the Ñorquin river, possibly due to sorption of this element onto Al hydroxides above pH 6 (Sánchez-España et al., 2006). On the other hand, Fe/Cl and Al/Cl present almost constant values along the system up to 30 km from the crater lake, after which some ratios start to show depleted values (Fig. 7a). In this way, Fe and Al transition from conservative to non-conservative behavior, this change occurs in Cavihue lake and, more evidently, in the lower Agrio river. At these points, these elements are involved in hydroxysulfate precipitation, and this behavior is recognized in the trend break in Fig. 7b (Gammons et al., 2005; Agosto and Varekamp, 2016; Rodríguez et al., 2016; Llano et al., 2020). Something similar occurs with As, V, and Cr, but with more variability (Fig. 7a and 7b).

The hydroxysulfates minerals that precipitate in the system are schwertmannite and basaluminite (Rodríguez et al., 2016; Llano et al., 2020). The former is an Fe hydroxysulfate ($\text{Fe}_8\text{O}_8(\text{OH})_x(\text{SO}_4)_y$; $8-x=2y$, $1 < y < 1.75$) with an amorphous structure and a high specific surface area on which some elements can be readily adsorbed (Bigham et al., 1996; Bigham and Nordstrom, 2000; Regenspurg and Peiffer, 2005). The chemical analysis of this mineral made in the study area show significant contents of As and V (Alexander, 2014; Rodríguez et al., 2016). The latter is an Al hydroxysulfate ($\text{Al}_4(\text{SO}_4)(\text{OH})_{10}$), which also has an amorphous internal structure, favoring the adsorption of trace elements on the precipitates due to its high specific surface area (Sánchez-España et al., 2016; Lozano et al., 2018). Schwertmannite precipitation occurs at pH above 3 (Caraballo et al., 2013; Rodríguez et al., 2016; Llano et al., 2020), whereas basaluminite precipitates at pH between 4 and 5 (Bigham and Nordstrom, 2000; Delmelle and Bernard, 2000; Sánchez-España et al., 2011; Llano et al., 2020). Notably, the precipitation process affects the cation but not the anion trends. Despite being an essential component of the hydroxysulfate minerals, a precipitation break is not recognized in the SO_4 dilution trend (Fig. 6b), likely because the amount of precipitate is relatively minor concerning the high concentrations of this anion in the VHS waters.

Therefore, two hypotheses are proposed to explain the sudden change of As, V, and Cr behavior (Fig. 7a and 7b): i) these elements are affected by adsorption as oxyanions onto the hydroxysulfate

minerals surfaces (Carlson et al., 2002; Jonsson et al., 2005; Regenspurg and Peiffer, 2005; Antelo et al., 2012; Sánchez-España et al., 2016), or ii) these elements as oxyanions partially replace the sulfate in the internal structure of the minerals (Fukushi et al., 2003; Regenspurg and Peiffer, 2005; Antelo et al., 2012).

5.3 Rare earth elements

REE patterns in natural water result from four main factors that depend on the pH and redox conditions (Lewis et al., 1997; Inguaggiato et al., 2015; Oliveri et al., 2019): i) the intensity of the water-rock interaction that defines the element concentration in the fluid; ii) the formation of complexes; iii) the incorporation of REE into the structure of secondary mineral precipitates; and iv) the adsorption of REE onto minerals surfaces. Particularly, in the CCVC rocks, the REE patterns normalize by chondrite are very similar to the normalized continental crust patterns (Varekamp et al., 2006; Roulleau et al., 2018).

The NASC normalized REE concentrations of water samples are shown in Fig. 8. The REE patterns for the VHS headwaters show in general a similar flat pattern, with a progressive depletion downstream (from site 1 to 11). In this upper part of the system, the incorporation of REE to the waters do not come only from REE-rich minerals, such as apatite or zircon, but rather from all minerals of the study area despite the REE concentrations (Grawunder et al., 2018; Migaszewski et al., 2019), as it is recognized in the rock compositions of CCVC (Varekamp et al., 2006; Roulleau et al., 2018). The Crater lake sample from Gammons et al. (2005) is flatter than both springs, due to a more congruent rock dissolution with a similar behavior in all the REE, without a fractionation during water-rock interaction. Nevertheless, a slight depletion in light REE can be recognized in the springs ($\text{La}_{\text{NASC}}/\text{Sm}_{\text{NASC}}$ of 0.92 for the South spring and 1.11 for the North spring), related to alunite and jarosite precipitation (Inguaggiato et al., 2015; Varekamp, 2015; Inguaggiato et al., 2017). This depletion in light REE is more evidenced in the SHW patterns ($\text{La}_{\text{NASC}}/\text{Sm}_{\text{NASC}}$ of: 0.57 in Agua del Limón, 0.29 in Las Maquinitas, and 0.44 in Las Máquinas), these waters being more affected by the adsorption of light REE onto secondary minerals such as alunite (Gammons et al.,

2005; Inguaggiato et al., 2015; Gaviria-Reyes et al., 2016). The heavy REE flat patterns for the three SHW samples (Gd_{NASC}/Lu_{NASC} of: 1.32 in Agua del Limón, 1.27 in Las Maquinitas, and 1.47 in Las Máquinas) indicate that they are not affected by the mentioned adsorption process. Although, being the SO_4 the main ligand present in the system, it is possible that a complexation control may be affecting the light REE concentrations and not the heavy REE (Lewis et al., 1997; Inguaggiato et al., 2015).

The negative Eu anomaly in Colorado stream (Site 19; Eu/Eu^* : 0.64), in Pucón Mahuida stream (Site 15; Eu/Eu^* : 0.62), and in the cold crater lake (Site 1; Eu/Eu^* : 0.75) can be explained by incongruent rock dissolution (Shakeri et al., 2015; Varekamp, 2015), whereas the more acidic and hotter waters present a lower negative anomaly (Table 3) due to a more congruent dissolution of the rock. This anomaly can also be explained by a selective co-precipitation of Eu with Fe oxyhydroxide minerals (Shakeri et al., 2015), being this the most probable explanation. The repetition of the VHS-patterns downstream shows the progressive dilution controlling REE concentrations, being evidenced also in the decreasing value of the Eu/Eu^* downstream (0.76 in the Salto del Agrio, site 11) due to the MW income (Table 2). The Pucón Mahuida stream pattern is similar to the Colorado stream pattern because of its proximity to the volcanic emission center and the interaction with volcanic ash, emitted during the current eruptive cycle that started in 2012 (Daga et al., 2017; Llano et al., 2020). The Ce/Ce^{IV} values indicate that none of the samples present an anomaly in this element, due to similar redox conditions in the system despite some minor variations in Eh values (Gammons et al., 2005; Rodriguez et al., 2016).

5.4 Geochemical conceptual model

The general processes described in the CCVC are represented in Fig. 9 as a geochemical conceptual model. Here, the magmatic source is located at ~5km (Velez et al., 2011) which emits magmatic gases that interact with two aquifers: an hyperacid brine located near the surface of Copahue volcano, and a geothermal aquifer located below the geothermal field.

Each group of water presents a particular trace element pattern, directly related to the processes that affect their composition. The MW are representative of the meteoric waters that recharge the regional system, whose normalized patterns are depleted in most of the elements compare to Na and only affected by hydroxide mineral precipitation at neutral pH. The hot and acidic VHS waters normalized patterns show enrichment comparing to Na in almost every element due to a more intense water-rock interaction, with some higher element values (Mg, Mn, Co, Ni, and Zn) favored by dissolution of fresh rock feeding into the source area during the current eruptive cycle. In particular, B, As, Cd, Se, Tl, and Te are enriched in this water group as a result of the magmatic gas contribution. On the other hand, Ba has very low ratios due to barite precipitation. The SHW show flatter normalized patterns than the VHS because in this part of the system there is no fresh rock available to leach out, and for this reason, water-rock interaction processes are more stable than in the VHS area.

It was also recognized that the dilution process developed along the Agrio river affects not only the major elements but most of the trace elements as well. But for some elements, like Na and Sr, input from MW tributaries to the Agrio river system is also important. Nevertheless, the decreasing pattern cannot be only ascribed to simple dilution. For Fe, Al, As, Cr, and V, schwertmannite and basaluminite precipitation is the primary control over the most depleted concentrations downstream. However, for As, Cr, and V it is still necessary to determine if these trace elements are incorporated in the internal structure of the Fe and Al hydroxysulfate minerals or simply adsorbed onto their surface.

The REE normalized patterns of the VHS group have slightly lower light REE ratios than heavy REE, possibly controlled by alunite and jarosite precipitation in the headwaters. The SHW group show similar patterns but with more depleted ratios in the light REE than in the VHS. The MW and the Colorado stream patterns have a negative Eu anomaly likely affected by co-precipitation with Fe hydroxide minerals.

Overall, our data highlight that some volatile elements are incorporated to the CCVC headwaters and geothermal field waters from the magmatic gases input. The same processes may act in other

Volcanic systems in Argentina and are still to be studied, being an important link between the deep magmatic chamber activity and the water bodies at the surface or circulating at various depths within the volcanic system.

6. Conclusions

This is the first study regarding trace element and REE behavior in all the CCVC waters. This work contributes to the knowledge of this active volcanic region with a detailed description and process evaluation for minor, trace, and REE composition of the different water groups of the system. The proposed hydrogeochemical model can explain the behavior of most of the analyzed species and elements present in the study area.

The main results of this study are the input through the magmatic gases and aerosols emissions of As, B, Tl, Cd, Se, and Te in the VHS waters and B and Cd in the geothermal field waters. Furthermore, all the described samples keep relatively similar patterns in both campaigns (2017 and 2018), even when the volcano was undergoing an eruptive period, showing significant stability in the system. Nevertheless, the absolute concentrations for the VHS headwaters and the SHW in 2018 were higher than for the 2017 campaign samples, probably related to higher contributions due to the increment in the volcano activity recognized by a diminution in the precipitations from 2016 to 2017.

The processes described in the system can be study in other volcano-hydrothermal systems of Argentina, such as Planchón-Peteroa Volcano, Domuyo volcanic complex, Deception Island, etc, in order to understand more about the behavior of trace elements related to volcanic activity. Finally, the chemical analysis of some trace elements as for example As or B, should be incorporated in future monitoring and surveillance programs of Copahue volcanic activity.

Funding

The research leading to these results has received funding from the projects UBACyT 20020150200230BA, UBACyT 20020170200221BA, PICT-2015-3110, PICT-2016-2624 and Proyecto de Unidad Ejecutora (IDEAN) 22920160100051. This is the R-447 contribution of the Instituto de Estudios Andinos “Don Pablo Groeber”.

Journal Pre-proof

- Agusto, M., 2011. Estudio geoquímico de los fluidos volcánicos e hidrotermales del Complejo volcánico Copahue Caviahue y su aplicación para tareas de seguimiento [Ph.D. Thesis]. University of Buenos Aires.
- Agusto, M., Caselli, A., Tassi, F., Dos Santos Afonso, M., Vaselli, O., 2012. Seguimiento geoquímico de las aguas ácidas del sistema volcán Copahue-Río Agrio: Posible aplicación para la identificación de precursores eruptivos. *Rev. Asoc. Geol. Argent.* 69, 481-495.
- Agusto, M., Tassi, F., Caselli, A., Vaselli, O., Rouwet, D., Capaccioni, B., Caliro, S., Chiodini, G., Darrah, T., 2013. Gas geochemistry of the magmatic-hydrothermal fluid reservoir in the Copahue-Caviahue Volcanic Complex (Argentina). *J. Volcanol. Geotherm. Res.* 257, 44-56.
- Agusto, M., Caselli, A., Daga, R., Varekamp, J., Trinelli, A., Dos Santos Afonso, M., Guevara, S.R., 2017. The Crater Lake of Copahue volcano (Argentina): geochemical and thermal changes between 1995 and 2015. *Geol. Soc. Lond., Spec. Publ.* (), 107–130.
- Agusto, M., Varekamp, J., 2016. The Copahue Volcanic-Hydrothermal System and Applications for Volcanic Surveillance. In: Tassi, F., Vaselli, O. and Caselli, A. (eds.), *Copahue Volcano, Active Volcanoes of the world Book Series*, Springer, Berlin-Heidelberg, pp 199-238.
- Agusto, M., Velez, L., 2017. Avances en el conocimiento del sistema volcánico-hidrotermal del Copahue: a 100 años del trabajo pionero de don Pablo Groeber. *Rev. Asoc. Geol. Argent.* 74 (1), 109-124.
- AIC (Autoridad Interjurisdiccional de las Cuencas de los Ríos Limay, Neuquén y Negro). 2017. *Anuario Hidrológico: Cuenca Activa de los ríos Limay y Neuquén.* 78 pp.
- AIC (Autoridad Interjurisdiccional de las Cuencas de los Ríos Limay, Neuquén y Negro). 2018. *Anuario Hidrológico: Cuenca Activa de los ríos Limay y Neuquén.* 78 pp.
- Aiuppa, A., Allard, P., D'Alessandro, W., Michel, A., Parello, F., Treuil, M., Valenza, M., 2000a. Mobility and fluxes of major, minor and trace metals during basalt weathering at Mt. Etna volcano (Sicily). *Geochim. Cosmochim. Acta* 64, 1827–1841.

- Aiuppa, A., Dongarra, G., Capasso, G., Allard, P., 2000. Trace elements in the thermal waters of Vulcano Island. *J. Volcanol. Geotherm. Res.* 98, 189–207.
- Aiuppa, A., Bellomo, S., Brusca, L., D'Alessandro, W., Federico, C., 2003. Natural and anthropogenic factors affecting groundwater quality of an active volcano (Mt. Etna, Italy). *Appl. Geochem.* 18 (6), 863-882.
- Aiuppa, A., Federico, C., Allard, P., Gurrieri, S., Valenza, M., 2005. Trace metal modeling of groundwater–gas–rock interactions in a volcanic aquifer: Mount Vesuvius, Southern Italy. *Chem. Geol.* 216 (3-4), 289-311.
- Ajouyed, O., Hurel, C., Ammari, M., Allal, L.B., Marmier, N., 2010. Sorption of Cr (VI) onto natural iron and aluminum (oxy) hydroxides: effects of pH, ionic strength and initial concentration. *J. Hazard. Mater.* 174 (1-3), 616-622.
- Albite, J.M., Vigide, N., Caselli, A., 2019. Caracterización de eventos glaciovolcánicos en el Complejo volcánico Cavihue-Copahue y en la Formación Hualcupén, provincia del Neuquén. *Rev. Asoc. Geol. Argent.* 76 (3), 183-198.
- Alexander, E., 2014. Aqueous geochemistry of an active magmato-hydrothermal system: Copahue Volcano, Río Agrio and Lake Cavihue, Neuquén, Argentina [B. Thesis]. Wesleyan University.
- Antelo, J., Fiol, S., Gondar, D., López, R., Arce, F., 2012. Comparison of arsenate, chromate and molybdate binding on schwertmannite: Surface adsorption vs anion-exchange. *J. C. Interface Sci.* 386(1), 338-343.
- Baes C.F., Mesmer R.E., 1976. Hydrolysis of cations. Wiley-Interscience, New York.
- Báez, A., Báez, W., Caselli, A., Martini, M., Sommer, C., 2020. The glaciovolcanic evolution of the Copahue volcano, andean southern volcanic zone, Argentina-Chile. *J. Volcanol. Geotherm. Res.* 396, 106866.
- Barcelona, H., Yagupsky, D., Agosto, M., 2019. The layered model of the Copahue geothermal reservoir, Argentina. *Geotherm. Energy* 7 (1), 1-22.
- Bia, G., Borgnino, L., Zampieri, G., Garcia, M.G., 2020. Fluorine surface speciation in South Andean volcanic ashes. *Chem. Geol.* 532, 119402.

- Bia, G., García, M.G., Cosentino, N., Doriggino, E., 2022. Dispersion of arsenic species from highly explosive historical volcanic eruptions in Patagonia. *Sci. Total Environ.* 853, 158389.
- Bigham, J.M., Schwertmann, U., Traina, S., Winland, R., Wolf, M., 1996. Schwertmannite and the chemical modeling of iron in acid sulfate waters. *Geochim. Cosmochim. Acta* 60, 2111-2121.
- Bigham, J.M., Nordstrom, D.K., 2000. Iron and Aluminum Hydroxysulfates from Acid Sulfate Waters. *Rev. Mineral. Geochem.* 40, 351-403.
- Benavente, O., Tassi, F., Reich, M., Aguilera, F., Capecchiacci, F., Gutiérrez, F., Vaselli, O., Rizzo, A., 2016. Chemical and isotopic features of cold and thermal fluids discharged in the Southern Volcanic Zone between 32.5 S and 36 S: Insights into the physical and chemical processes controlling fluid geochemistry in geothermal systems of Central Chile. *Chem. Geol.* 420, 97-113.
- Cabrera, J.M., Diaz, M.M., Schultz, S., Temporetti, P., Pedrero, F., 2016. Iron buffer system in the watercolumn and partitioning in the sediments of the naturally acidic Lake Caviabue, Neuquén, Argentina. *J. Volcanol. Geotherm. Res.* 318, 19-26.
- Calabrese, S., Aiuppa, A., Allard, P., Bagnato, E., Bellomo, S., Brusca, L., D'Alessandro, W., Parello, F., 2011. Atmospheric sources and sinks of volcanogenic elements in a basaltic volcano (Etna, Italy). *Geochim. Cosmochim. Acta* 75 (23), 7401-7425.
- Candela-Becerra, L.J., Toyos, C., Suárez-Herrera, C.A., Castro-Godoy, S., Agosto, M., 2020. Thermal evolution of the Crater Lake of Copahue Volcano with ASTER during the last quiescence period between 2000 and 2012 eruptions. *J. Volcanol. Geotherm. Res.* 392, 106752.
- Caraballo, M., Rimstidt, D., Macías, F., Nieto, J.M., Hochella, Jr.M., 2013. Metastability, nanocrystallinity and pseudo-solid solution effects on the understanding of schwertmannite solubility. *Chem. Geol.* 360, 22-31.
- Carlson, L., Bigham, J. M., Schwertmann, U., Kyek, A., Wagner, F., 2002. Scavenging of As from acid mine drainage by schwertmannite and ferrihydrite: a comparison with synthetic analogues. *Environ. Sci Technol.* 36 (8), 1712-1719.

- Caselli, A., Agosto, M., Velez, M.E., Forte, F., Bengoa, C., Daga, R., Ribero, J.M., Capaccioni, D., 2016. The 2012 eruption. In: Tassi, F., Vaselli, O., Caselli, A. (Eds.), Copahue Volcano. Active Volcanoes of the World. Springer, Berlin, Heidelberg, pp. 61–77.
- Cembrano, J., Lara, L., 2009. The link between volcanism and tectonics in the southern volcanic zone of the Chilean Andes: a review. *Tectonophysics*, 471 (1-2), 96-113.
- Chiacchiarini, P., Lavalle, L., Giaveno, A., Donati, E., 2010. First assessment of acidophilic microorganisms from geothermal Copahue–Caviahue system. *Hydrometallurgy* 104 (3-4), 334-341.
- D'Alessandro, W., Federico, C., Longo, M., Parello, F., 2004. Oxygen isotope composition of natural waters in the Mt Etna area. *J. Hydrol.* 296, 282-299.
- Daga, R., Caselli, A., Ribeiro Guevara, S., Agosto, M., 2017. Notas emitidas durante la fase inicial hidromagmática (julio de 2012) del ciclo eruptivo 2012-actual (2016) del volcán Copahue (Andes del sur). *Rev. Asoc. Geol. Argent.* 74 (2), 191-206.
- Deely, J.M., Sheppard, D.S., 1996. Whangaehu River, New Zealand: geochemistry of a river discharging from an active crater lake. *Appl. Geochem.* 11(3), 447-460.
- Delmelle, P., Bernard, A., Kusakabe, M., Fischer, T.P., Takano, B., 2000. Geochemistry of the magmatic–hydrothermal system of Kawah Ijen volcano, East Java, Indonesia. *J. Volcanol. Geotherm. Res.* 97 (1-4), 31-53.
- Delmelle, P., Bernard, A., 2000. Downstream composition changes of acidic volcanic waters discharged into the Banyuwangi stream, Ijen caldera, Indonesia. *J. Volcanol. Geotherm. Res.* 97 (1-4), 55-75.
- Delpino, D., Bermúdez, A., 1993. La actividad del volcán Copahue durante 1992. Erupción con emisión de azufre piroclástico. Provincia de Neuquén. 12° Congreso Geológico Argentino, Actas 4: 292-301, Mendoza.
- Delpino, D., Bermúdez, A., 2002. La erupción del volcán Copahue del año 2000. Impacto social y al medio natural. Provincia del Neuquén, Argentina. 15° Congreso Geológico Argentino, Actas 3: 365-370, El Calafate.

- Enzalde-Gonzalez, M.T., Matusch, J., Emmer, W.D., Wehmen, R., 2001. Sorption on natural solids for arsenic removal. *Chem. Eng. J.* 81, 187-195.
- Farnfield, H.R., Marcilla, A.L., Ward, N.I., 2012. Arsenic speciation and trace element analysis of the volcanic río Agrio and the geothermal waters of Copahue, Argentina. *Sci. Total Environ.* 433, 371-378.
- Fukushi, K., Sasaki, M., Sato, T., Yanase, N., Amano, H., Ikeda, H., 2003. A natural attenuation of arsenic in drainage from an abandoned arsenic mine dump. *Appl. Geochem.* 18 (8), 1267-1278.
- Gammons, C.H., Wood, S.A., Pedrozo, F., Varekamp, J., Nelson, B.J., Shope, C., Baffico, G., 2005. Hydrogeochemistry and rare earth element behavior in a volcanically acidified watershed in Patagonia, Argentina. *Chem. Geol.* 222, 249-267.
- Gaviria Reyes, M.A., Agosto, M., Trinelli, M.A., Caselli, A., dos Santos Afonso, M., Calabrese, S., 2016. Estudio hidrogeoquímico de las áreas termales del complejo volcánico Copahue-Caviahue. *Rev. Asoc. Geol. Argent.* 73, 256-269.
- Giggenbach, W.F., 1992. Isotopic shifts in waters from geothermal and volcanic systems along convergent plate boundaries and their origin. *Earth Planet. Sci. Lett.* 113, 495–510.
- Grawunder, A., Merten, D., Büchel, G., 2014. Origin of middle rare earth element enrichment in acid mine drainage-impacted area. *Environ. Sci. Pollut. Res.* 21, 6812-6823.
- Grawunder, A., Lonschinski, M., Pändel, M., Wagner, S., Merten, D., Mirgorodsky, D., Büchel, G., 2018. Rare earth element patterns as process indicators at the water–solid interface of a post–mining area. *Appl. Geochemistry* 96, 138-154.
- Gromet, L.P., Haskin, L.A., Korotev, R.L., Dymek, R.F., 1984. The “North American shale composite”: Its compilation, major and trace element characteristics. *Geochim. Cosmochim. Acta* 48 (12), 2469-2482.
- Guan, X.H., Wang, J., Chusuei, C.C., 2008. Removal of arsenic from water using granular ferric hydroxide: macroscopic and microscopic studies. *J. Hazardous Mater.* 156, 178-185.

- Hantush, M., Lacanna, G., Ripepe, M., Montenegro, V., Valderama, G., Panas, C., 2021. Low-energy fragmentation dynamics at Copahue Volcano (Argentina) as revealed by an infrasonic array and ash characteristics. *Front. Earth Sci.* 9, 578437.
- Inguaggiato, C., Censi, P., Zuddas, P., Londono, J.M., Chacon, Z., Alzate, D., Brusca, L., D'Alessandro, W., 2015. Geochemistry of REE, Zr and Hf in a wide range of pH and water composition: The Nevado del Ruiz volcano-hydrothermal system (Colombia). *Chem. Geol.* 417, 125-133.
- Inguaggiato, C., Burbano, V., Rouwet, D., Garzón, G., 2017. Geochemical processes assessed by Rare Earth Elements fractionation at “Laguna Verde” acidic-sulphate crater lake (Azufral volcano, Colombia). *Appl. Geochem.* 79, 65-74.
- Inostroza, M., Moune, S., Moretti, R., Burckel, P., Chilin-Eusebe, E., Dessert, C., Robert, V., Gorge, C., 2023. Major and trace element emission rates in hydrothermal plumes in a tropical environment. The case of La Soufrière de Guadeloupe volcano. *Chem. Geol.* 632, 121552.
- Jönsson, J., Persson, P., Sjöberg, S., Lövgren, L., 2005. Schwertmannite precipitated from acid mine drainage: phase transformation, sulfate release and surface properties. *Appl. Geochem.* 20, 179-191.
- Kusakabe, M., Komoda, Y., Takano, F., Abiko, T., 2000. Sulfur isotopic effects in the disproportionation reaction of sulfur dioxide in hydrothermal fluids: implications for the $\delta^{34}\text{S}$ variations of dissolved bisulfate and elemental sulfur from active crater lakes. *J. Volcanol. Geotherm. Res.* 97, 287-307.
- Lamberti, M.C., Vigide, N., Venturi, S., Agosto, M., Yagupsky, D., Winocur, D., Barcelona, H., Velez, M.L., Cardellini, C., Tassi, F., 2019. Structural architecture releasing deep-sourced carbon dioxide diffuse degassing at the Caviabue-Copahue Volcanic Complex. *J. Volcanol. Geotherm. Res.* 374, 131-141.
- Lewis, A.J., Palmer, M.R., Sturchio, N.C., Kemp, A.J., 1997. The rare earth element geochemistry of acid-sulphate and acid-sulphate-chloride geothermal systems from Yellowstone National Park, Wyoming, USA. *Geochim. Cosmochim. Acta.* 61 (4), 695-706.

- Linares, L., Osteria, H., Mas, L., 1999. Cronología Rb-Sr del Complejo Erusivo Copahue-Caviahue, Provincia del Neuquén. *Rev. Asoc. Geol. Argent.* 54, 240-247.
- Liotta, M., D'Alessandro, W., Bellomo, S., Brusca, L., 2016. Volcanic plume fingerprint in the groundwater of a persistently degassing basaltic volcano: Mt. Etna. *Chem. Geol.* 433, 68-80.
- Llano, J., Agosto, M., Trinelli, M.A., Tufo, A., García, S., Velásquez, G., Bucarey-Parra, C., Delgado Huertas, A., Litvak, V., 2020. Procesos hidrogeoquímicos vinculados a un ambiente volcánico activo: el caso del sistema río Agrio-Volcán Copahue. *Rev. Asoc. Geol. Argent.* 77, 490-504.
- Llano, J., Lamberti, M. C., Sierra, D., Agosto, M., 2021. Hydrogeochemistry of an Acid River and Lake Related to an Active Volcano. The Case of Study: Agrio River-Copahue Volcano in Patagonia, Argentina. In: *Environmental Assessment of Patagonia's Water Resources* (pp. 75-94). Springer, Cham.
- Lozano, A., Fernández-Martínez, A., Ayora, C., Paulán, A., 2018. Local structure and ageing of basaluminite at different pH values and sulphate concentrations. *Chem. Geol.* 496, 25-33.
- Mas, G.R., Mas, L.C., Bengochea, L., 1996. Alteración ácido-sulfática en el Campo Geotérmico Copahue, Provincia del Neuquén. *Rev. Asoc. Geol. Argent.* 51, 78-86.
- Melnick, D., Folguera, A., Ramo, V., 2006. Structural control on arc volcanism: The Cavihue-Copahue complex, Central to Patagonian Andes transition (38°S). *J. S. Am. Earth Sci.* 22, 66-88.
- Migaszewski, Z. M., Gałuszka, A., Dołęgowska, S., 2016. Rare earth and trace element signatures for assessing an impact of rock mining and processing on the environment: Wiśniówka case study, south-central Poland. *Environ. Sci. Pollut. Res.* 23, 24943-24959.
- Migaszewski, Z. M., Gałuszka, A., Dołęgowska, S., 2019. Extreme enrichment of arsenic and rare earth elements in acid mine drainage: case study of Wiśniówka mining area (south-central Poland). *Environ. Pollut.* 244, 898-906.
- Muñoz, J., Stern, C.R., 1988. The Quaternary volcanic belt of the southern continental margin of South America: transverse structural and petrochemical variations across the segment between 38 S and 39 S. *J. S. Am. Earth Sci.* 1(2), 147-161.

- Naciri, A., Westermann, T., Mustafa, S., 2007. Vanadium removal by metal (hydr) oxide adsorbents. *Water Res.* 41 (7), 1596-1602.
- Naranjo, J., Polanco, E., 2004. The 2000 AD eruption of Copahue Volcano, Southern Andes. *Rev. Geo. Chile* 31, 279-292.
- Oliveri, Y., Cangemi, M., Capasso, G., Saiano, F., 2019. Pathways and fate of REE in the shallow hydrothermal aquifer of Vulcano island (Italy). *Chem. Geol.* 512, 121-129.
- Paez, P.A., Cogliati, M.G., Caselli, A., Monasterio, A., 2021. An analysis of volcanic SO₂ and ash emissions from Copahue volcano. *J. S. Am. Earth Sci.* 110, 103365.
- Palmer, S., van Hinsberg, V., McKenzie, J., Yee, S., 2011. Characterization of acid river dilution and associated trace element behavior through hydrogeochemical modeling: A case study of the Banyu Pahit River in East Java, Indonesia. *Appl. Geochem.* 26, 1802-1810.
- Panarello, H., 2002. Características isotópicas y termodinámicas de reservorio del campo geotérmico Copahue-Caviahue, provincia de Neuquén. *Rev. Asoc. Geol. Argent.* 57, 182-194.
- Parker, S., Gammons, C., Pedrozo, F., Wood, S., 2008. Diel changes in metal concentrations in a geogenically acidic river: Río Agrio, Argentina. *J. Volcanol. Geotherm. Res.* 178, 213-223.
- Parkhurst, D., Appelo, C., 2013. Description of input and examples for PHREEQC version 3-A computer program for speciation, batch-reaction, one-dimensional transport and inverse geochemical calculations. U.S. Geological Survey Techniques and Methods 6, 497 p., Denver.
- Petrinovic, I., Villarosa, C., Delia, L., Guzman, S., Paez, G., Outes, V., Manzoni, C., Delmenico, A., Balbis, C., Carniel, R., Hernando, I., 2014. La erupción del 22 de diciembre de 2012 del volcán Copahue, Neuquén, Argentina: Caracterización del ciclo eruptivo y sus productos. *Rev. Asoc. Geol. Argent.* 71, 161-173.
- Regenspurg, S., Peiffer, S., 2005. Arsenate and chromate incorporation in schwertmannite. *Appl. Geochem.* 20, 1226-1239.
- Rodriguez, A., Varekamp, J., van Bergen, M., Kading, T., Oonk, P., Gammons, C., Gilmore, M., 2016. Acid Rivers and Lakes at Caviahue-Copahue Volcano as Potential Terrestrial Analogues for

Volcano, Active Volcanoes of the world Book Series, Springer, Berlin-Heidelberg, pp. 141-172.

Romero-Mujalli, G., Hartmann, J., Hosono, T., Louvat, P., Okamura, K., Delmelle, P., Amann, T., Böttcher, M.E., 2022. Hydrothermal and magmatic contributions to surface waters in the Aso caldera, southern Japan: Implications for weathering processes in volcanic areas. *Chem. Geol.* 588, 120612.

Rouilleau, E., Tardani, D., Sano, Y., Takahata, N., Vinet, N., Bravo, F., Muñoz, C., Sanchez, J., 2016. New insight from noble gas and stable isotopes of geothermal/hydrothermal fluids at Cavihue-Copahue Volcanic Complex: boiling steam separation and water-rock interaction at shallow depth. *J. Volcanol. Geotherm. Res.* 328, 70–83.

Rouilleau, E., Tardani, D., Vlastelic, I., Vinet, N., Sanchez, J., Sano, Y., Takahata, N., 2018. Multi-element isotopic evolution of magmatic rocks from Cavihue-Copahue Volcanic Complex (Chile-Argentina): Involvement of mature slab recycled materials. *Chem. Geol.* 476, 370-388.

Rouwet, D., Hidalgo, S., Joseph, E.P., González-Ilama, G., 2017. Fluid geochemistry and volcanic unrest: dissolving the haze in time and space. In: Gottsmann, J., Neuberg, J., Sheu, B. (eds), *Advances in volcanology*. Springer, Berlin-Heidelberg, 221-239.

Rowe, Jr.G.L., 1994. Oxygen, hydrogen, and sulfur isotope systematics of the crater lake system of Poas volcano, Costa Rica. *Geochim. J.* 28 (3), 263-287.

Sánchez-España, J., Pardo, L.L., Pastor, E.S., Andrés, J.R., Rubí, J.A., 2006. The removal of dissolved metals by hydroxysulphate precipitates during oxidation and neutralization of acid mine waters, Iberian Pyrite Belt. *Aquat. Geochem.* 12 (3), 269-298.

Sánchez-España, J., Yusta, I., Díez-Ercilla, M., 2011. Schwermannite and hydrobasaluminite: A re-evaluation of their solubility and control on the iron and aluminium concentration in acidic pit lakes. *Appl. Geochem.* 26, 1752-1774.

Sánchez-España, J., Yusta, I., Gray, J., Burgos, W.D., 2016. Geochemistry of dissolved aluminum at low pH: Extent and significance of Al-Fe (III) coprecipitation below pH 4.0. *Geochimica et Cosmochimica Acta* 175, 128-149.

- Straoza, F., Tamm, M., Corvado, M., Kaufman, J., Lissondo, M., Craig, V., Dadi, G., Garcia, S., 2021. Late Pleistocene subglacial fissure-related volcanism at Caviahue-Copahue Volcanic Complex (37° 51' S, 71° 05' W), South Volcanic Zone. *J. S. Am. Earth Sci.* 110, 103309.
- Scholtysik, R., Canil, D., 2018. Condensation behaviour of volatile trace metals in laboratory benchtop fumarole experiments. *Chem. Geol.* 492, 49-58.
- Shakeri, A., Ghoreyshinia, S., Mehrabi, B., Delavari, M., 2015. Rare earth elements geochemistry in springs from Taftan geothermal area SE Iran. *J. Volcanol. Geotherm. Res.* 304, 49-61.
- Stumm, W., Morgan, J.J., 1996. Aquatic chemistry: Chemical equilibria and rates in natural waters. Wiley-Interscience publication, New York.
- Taran, Y., Rouwet, D., Inguaggiato, S., Aiuppa, A., 2008. Major and trace element geochemistry of neutral and acidic thermal springs at El Chichón volcano, Mexico: implications for monitoring of the volcanic activity. *J. Volcanol. Geotherm. Res.* 178 (2), 224-236.
- Tardani, D., Roulleau, E., Pinti, D.L., Pérez-Flóres, P., Daniele, L., Reich, M., Sanchez-Alfaro, P., Morata, D., Richard, L., 2021. Structural control on shallow hydrogeochemical processes at Caviahue-Copahue Volcanic Complex (CCVC), Argentina. *J. Volcanol. Geotherm. Res.* 414, 107228.
- Tassi, F., Aguilera, F., Benavente, O., Faonita, A., Chiodini, G., Caliro, S., Agosto, M., Gutierrez, F., Capaccioni, B., Vaselli, O., Caselli, A., Saltori, O., 2016. Geochemistry of fluid discharges from Peteroa volcano (Argentina-Chile) in 2010–2015: Insights into compositional changes related to the fluid source region (s). *Chem. Geol.* 432, 41-53.
- Tassi, F., Agosto, M., Lamberti, C., Caselli, A., Pecoraino, G., Caponi, C., Szentiványi, J., Venturi, S., Vaselli, O., 2017. The 2012-2016 eruptive cycle at Copahue volcano (Argentina) versus the peripheral gas manifestations: hints from the chemical and isotopic features of fumarolic fluids. *Bull. Volcanol.* 79 (10), 1-14.
- Varekamp, J.C., 2008. The volcanic acidification of glacial Lake Caviahue, province of Neuquén, Argentina. *J. Volcanol. Geotherm. Res.* 178 (2), 184-196.

- Varekamp, J.C., 2015. The chemical composition and evolution of volcanic lakes. In: Rouwet, D., Christenson, B., Tassi, F., Vandemeulebrouck, J. (Eds.), Volcanic Lakes. Advances in Volcanology, Springer-Verlag, pp. 93–123.
- Varekamp, J.C., de Moor, J.M., Merrill, M.D., Colvin, A.S., Goss, A.R., Vroon, P.Z., Hilton, D.R., 2006. Geochemistry and isotopic characteristics of the Caviahue-Copahue volcanic complex, Province of Neuquén, Argentina. *Geol. Soc. Am. Spec. Pap.* 407, 317–342.
- Varekamp, J., Ouimeete, A., Herman, S., Flynn, K., Bermúdez, A., Delpino, D., 2009. Naturally acid waters from Copahue volcano, Argentina. *Appl. Geochem.* 24, 208–220.
- Velez, M.L., Euillades, P., Caselli, A., Blanco, M., Díaz, J.M., 2011. Deformation of Copahue volcano: inversion of InSAR data using a genetic algorithm. *J. Volcanol. Geotherm. Res.* 202 (1–2), 117–126.
- Wedepohl, K.H., 1995. The composition of the continental crust. *Geochim. Cosmochim. Acta* 59 (7), 1217–1232.
- Wrage, J., Tardani, D., Reich, M., Daniel, I., Arancibia, G., Cembrano, J., Sánchez-Alfaro, P., Morata, D., Pérez-Moreno, R., 2017. Geochemistry of thermal waters in the Southern Volcanic Zone, Chile - Implications for structural controls on geothermal fluid composition. *Chem. Geol.* 466, 545–561.

Fig. 1: Location of the Caviahue-Copahue Volcanic Complex and water groups of the area with the sampling sites.

Fig. 2: a) Copahue volcano crater in 2018 where are recognized a hot and a cold crater lakes (Site 1). b) View to the east from the crater where are recognized the springs (Sites 2 and 3), upper Agrio river (Sites 4, 5, 6, 7, and 8), Caviahue lake (Site 9) and Las Mellizas lakes (Site 18). c) Caviahue lake (Site 9). d) Pucón Mahuida stream (Site 15). e) Trolope river (Site 16). f) Las Máquinas (Site 20). g) Las Maquinitas (Site 21).

Fig. 3: Ternary diagrams for major anions and cations composition. Rocks composition was taken from Roulleau et al. (2018).

Fig. 4: Sulfate and element concentrations in $\mu\text{g/L}$ for Trolope river (MW), South spring (VHS), and Las Máquinas (SHW). Elements are arranged for decreasing values at Trolope river.

Fig. 5: Major cations and trace element concentrations of melt waters (MW), volcanic hydrological system (VHS), and steam heated waters (SHW) samples normalized by an average rock composition (Roulleau et al., 2018). Samples of the 2017 and 2018 campaigns are distinguished.

Fig. 6: a) Metal/chloride ratios versus distance (km) from the crater lake. b) Elements versus Cl concentrations ($\mu\text{g/L}$). Blue circles correspond to VHS; light blue circles correspond to MW; blue and light blue x symbols correspond to VHS and MW, respectively, from other authors' data (Gammons et al., 2005; Parker et al., 2008; Chiacchiarini et al., 2010; Augusto et al., 2012; Alexander, 2014; Augusto and Varekamp, 2016; Rodriguez et al., 2016). Upper Agrio river, Caviahue lake, and lower Agrio river zones are distinguished by shading.

Fig. 7: a) Metal/chloride ratios versus distance (km) from the crater lake. b) Elements versus Cl concentrations ($\mu\text{g/L}$).

Fig. 8: REE concentrations of the VHS waters, MW, and SHW normalized by NASC (Gromet et al., 1984).

Fig. 9: Schematic model of the Caviahue-Copahue Volcanic Complex hydrological system and its processes.

Table 1. Chemical compositions of the 2017 and 2018 samples.

Site	Sample	Group	Date	T	pH	EC	HCO ₃	SO ₄	Cl	F	Na	K	Ca	Mg	Fe	Si	Al
1	Crater lake (cold lake)	MW	27/02/2018	8	3.5	280	n.d.	62	18	n.a.	2.20	12	8.80	7.20	4.67	2.07	3.23
2	South spring	VHS	14/02/2017	19	2.9	n.a.	n.d.	1613	491	71	85	9.00	190	310	89	n.a.	112
2	South spring	VHS	27/02/2018	32	1.9	>20000	n.d.	10926	5964	n.a.	564	55	679	1756	1036	156	716
3	North spring	VHS	14/02/2017	19, 1	1.8	n.a.	n.d.	4043	1982	177	240	9.00	670	545	320	n.a.	288
3	North spring	VHS	27/02/2018	27	2.0	17000	n.d.	6523	3333	n.a.	324	90	598	967	760	74	572
4	Upper Agrio river (Higher site)	VHS	12/02/2017	19	2.7	2500	n.d.	1721	660	41	140	18	255	240	83	n.a.	105
5	Upper Agrio river (Ski station)	VHS	12/02/2017	22	3.0	n.a.	n.d.	1874	621	35	145	18	300	300	84	n.a.	89
5	Upper Agrio river (Ski station)	VHS	02/03/2018	17	2.0	17500	n.d.	16735	3496	n.a.	368	40	552	1125	834	112	528
6	Upper Agrio river (After Pucón Mahuida stream)	VHS	12/02/2017	15	3.7	n.a.	n.d.	666	227	8.40	48	9.80	106	105	16	n.a.	22
7	Upper Agrio river (Sismic station)	VHS	12/02/2017	21	3.2	n.a.	n.d.	694	236	9.2	49	10	105	108	11.0	n.a.	21
8	Upper Agrio river (Bridge)	VHS	12/02/2017	23	3.2	n.a.	n.d.	535	178	7.10	40	8.80	83	84	6.70	n.a.	16
8	Upper Agrio river (Bridge)	VHS	28/02/2018	20	2.8	3170	n.d.	1699	790	n.a.	94	11	166	285	189	49	192
9	Caviahue lake	VHS	12/02/2017	23	2.3	n.a.	n.d.	253	76	4.70	14	5.00	25	23	13	n.a.	18
9	Caviahue lake	VHS	28/02/2018	20	3.1	870	n.d.	215	67	n.a.	13	3.90	23	22	7.00	16	14
10	Lower Agrio river (Bridge)	VHS	17/02/2017	14	2.8	402	n.d.	202	61	n.a.	12	4.60	19	16	1.49	15	13
10	Lower Agrio river (Bridge)	VHS	26/02/2018	21	2.8	670	n.d.	183	56	n.a.	12	3.60	21	19	2.09	n.a.	7.32
11	Lower Agrio river (Salto del Agrio)	VHS	17/02/2017	11	6.4	129	n.a.	53	17	0.73	7.30	3.10	12	8.3	0.054	9.33	0.038

11	Lower Agrio river (Salto del Agrio)	VHS	26/02/2018	20	3.7	320	n.d.	100	29	n.a.	8.0 0	2.5 0	15	12	0.67	12	18
12	Lower Agrio river (Puerta Trolope)	VHS	17/02/2017	16	5.1	189	n.d.	70	21	0.76	11	4.7 0	15	9.70	0.02 9	14	0.47
12	Lower Agrio river (Puerta Trolope)	VHS	28/02/2018	20	4.2	350	n.d.	93	29	n.a.	7.6 0	2.4 0	14	10	0.10	n.a.	6.46
13	Lower Agrio river (Before Ñorquin river)	VHS	17/02/2017	14	7.0	166	10	77	23	0.81	9.5 0	4.9 0	24	12	0.03 0	21	0.11
14	Lower Agrio river (After Ñorquin river)	VHS	17/02/2017	16	7.6	156	23	67	20	0.75	11	4.3 0	26	13	0.03 3	21	0.13
15	Pucón Mahuida stream	MW	12/02/2017	11	5.5	n.a.	n.d.	264	77	1.90	21	6.4 0	51	48	0.20	n.a.	1.38
15	Pucón Mahuida stream	MW	02/03/2018	13	5.9	800	83	112	98	2.80	22	6.1 0	58	55	0.37	22	1.73
16	Trolope river	MW	17/02/2017	11	7.4	95	31	12	4.5	0.18	4.9 0	1.9 0	7.5 0	5.10	0.12	5.6 0	0.01 0
16	Trolope river	MW	26/02/2018	25	6.1	96	29	7.50	2.10	0.12	2.8 0	0.8 0	5.7 0	3.10	0.07 1	n.a.	0.00 9
17	Ñorquin river	MW	17/02/2017	18	8.6	200	119	28	9.80	0.41	15	3.5 0	31	14	0.03 1	20	0.02 1
18	Las Mellizas lake	MW	26/02/2018	14	7.9	490	14	155	42	1.30	16	3.7 0	29	24	0.02 1	n.a.	0.07 7
19	Colorado stream	VHS	12/02/2017	26	3.2	n.a.	n.d.	2581	837	14	200	37	425	480	82	n.a.	13
19	Colorado stream	VHS	02/03/2018	19	3.7	3310	n.d.	1226	427	n.a.	102	24	291	257	33	30	179
20	Las Máquinas	SHW	13/02/2017	46	1.8	n.a.	n.d.	825	33	1.60	22	6.8 0	36	26	6.70	n.a.	9.66
20	Las Máquinas	SHW	26/02/2018	53	1.5	2430	n.d.	795	25	n.d.	12	4.0 0	28	16	13	37	11
21	Las Maquinillas	SHW	13/02/2017	63	1.9	n.a.	n.d.	1785	0.10	2.10	23	14	15	4.60	17	n.a.	32
21	Las Maquinillas	SHW	26/02/2018	82	1.7	4650	n.d.	4458	n.d.	n.d.	21	18	58	5.00	112	204	158
22	Agua del Limón	SHW	13/02/2017	73	1.7	n.a.	n.d.	1364	9.20	n.d.	24	14	17	6.20	24	n.a.	20
22	Agua del Limón	SHW	26/02/2018	61	1.8	3770	n.d.	1512	n.d.	n.d.	18	6.0 0	22	3.50	37	119	24
23	Anfiteatro	SHW	26/02/2018	27	6.2	190	33	21	n.a.	0.08 0	7.0 0	1.2	12	4.90	1.00	n.a.	0.05 1

Average rock composition (Rouleau et al., 2018)	Rock sample	-	-	-	-	-	-	-	-	-	3.75	2.02	7.11	3.87	8.38	-	16.8
---	-------------	---	---	---	---	---	---	---	---	---	------	------	------	------	------	---	------

Temperature (T) are in °C, electrical conductivity (EC) are in $\mu\text{S}/\text{cm}$, and ion concentrations are in mg/L . n.a. is not

analyzed, n.d. is not detected. VHS: Volcanic hydrological system; SHW: Steam heated water; MW: Melt waters. The average rock composition (Rouleau et al., 2018) concentrations are in oxide weight %.

Table 2: Trace elements concentrations for the 2017 and 2018 samples and an average rock composition (Rouleau et al., 2018).

Site	Sample	Group	Date	As	B	Ba	Be	Bi	Cd	Co	Cr	Cs	Cu	Hf	Li	Mn	Mo	Ni	Pb	Rb	Sr	Sr	Sr	Ta	Te	Th	Ti	Tl	U	V	Y	Zn	Zr
1	Crater lake (cold lake)	MW	27/02/2018	1.04	8.44	16.5	0.048	0.011	0.56	6.01	0.84	0.049	51.5	0.005	2.63	213	0.025	9.93	0.15	2.54	0.3	n.d.	34	n.d.	0.28	0.043	6.52	1.08	0.095	1.38	1.87	35.1	0.18
2	South spring	VHS	14/02/2017	42.3	76.6	5.88	2.85	0.11	17.9	15.6	23.1	1.17	33.1	n.a.	71.1	678	0.55	2.5	0.4	45.0	13.7	0.22	97.3	n.d.	1.60	n.a.	32.0	14.8	1.51	36.1	n.a.	52.4	n.a.
2	South spring	VHS	27/02/2018	29.22	14.11	0.20	14.7	0.053	56.7	24.2	21.2	17.7	21.9	0.23	55.4	56.1	0.28	50.5	n.d.	44.48	9.47	n.d.	46.66	0.095	4.64	11.6	44.4	65.2	5.92	14.97	52.5	44.40	3.67
3	North spring	VHS	14/02/2017	84.6	48.1	21.0	8.27	0.15	26.4	12.9	59.8	5.10	22.1	n.a.	20.9	168	0.45	21.6	71.2	13.7	3.87	0.259	n.a.	0.28	n.a.	11.7	25.6	1.75	47.4	n.a.	12.59	n.a.	
3	North spring	VHS	27/02/2018	12.98	92.9	0.12	8.65	0.029	39.0	94	12.4	8.81	10.4	0.17	57.8	339	n.d.	21.8	n.d.	21.0	4.07	n.d.	47.52	0.069	1.04	8.37	91.9	30.9	2.20	85.0	30.7	26.36	3.08
4	Upper Agrio river (Higher site)	VHS	12/02/2017	33.9	23.4	9.49	5.91	0.016	4.00	16.1	10.6	2.8	24.1	n.a.	15.4	169	0.31	18.7	1.60	61.9	0.77	0.10	98.0	n.a.	0.19	n.a.	37.4	3.51	1.45	63.0	n.a.	33.7	n.a.
5	Upper Agrio river (Ski station)	VHS	12/02/2017	17.9	28.7	9.83	5.89	0.017	5.43	7.8	8.48	2.76	19.1	n.a.	19.6	233	0.36	20.1	0.69	75.9	1.22	0.057	10.48	n.a.	0.15	n.a.	29.8	2.95	1.27	39.4	n.a.	27.5	n.a.
5	Upper Agrio river (Ski station)	VHS	02/03/2018	20.09	95.4	0.10	10.5	0.035	38.3	19.3	15.1	11.4	16.7	0.17	41.7	397	0.45	39.8	n.d.	30.1	7.10	n.d.	39.27	0.065	2.37	8.26	29.1	47.4	3.81	13.09	37.9	29.48	2.11
6	Upper Agrio river (After Pucón Mahui da stream)	VHS	12/02/2017	1.15	91.5	11.5	1.62	0.012	1.14	50.1	1.82	1.77	11.2	n.a.	58.5	668	0.05	62.6	0.12	33.4	0.80	0.049	40.3	n.a.	0.054	n.a.	6.68	0.93	0.45	0.72	n.a.	85.7	n.a.
7	Upper Agrio river (Sismic station)	VHS	12/02/2017	1.62	10.1	10.5	1.61	0.008	1.43	49.6	0.97	1.85	15.1	n.a.	58.2	233	1.83	62.1	0.18	33.7	0.65	0.073	41.3	n.a.	0.051	n.a.	5.48	1.43	0.42	0.20	n.a.	85.9	n.a.
8	Upper Agrio river (Bridge)	VHS	12/02/2017	1.40	87.5	12.4	1.16	0.007	3.14	38.8	1.15	1.62	9.55	n.a.	47.3	532	0.62	49.0	0.17	31.8	0.52	0.037	36.2	n.a.	0.068	n.a.	7.00	2.11	0.28	0.48	n.a.	66.9	n.a.
8	Upper Agrio river (Bridge)	VHS	28/02/2018	26.0	21.9	13.5	2.49	0.012	8.49	65.4	26.0	3.28	51.5	0.047	11.1	120	0.44	10.8	12.6	81.5	1.57	0.32	10.06	0.014	0.44	1.57	66.0	11.4	0.87	24.1	91.9	65.5	0.49
9	Caviahue lake	VHS	12/02/2017	10.4	28.8	14.4	0.55	0.008	0.64	9.05	8.85	0.61	7.04	n.a.	12.6	105	0.11	14.3	4.09	15.5	0.49	0.081	17.4	n.a.	0.12	n.a.	24.3	2.24	0.28	16.5	n.a.	39.6	n.a.

9	Carman ue lake	VH S	20/02/ 2018	38	2	7	9		5	29	2	6	00	05	1	2	2	5	7	7	0		9		0	6	82	3	0	5	56	1	6
10	Lower Agrio river (Bridge)	VH S	17/02/ 2017	0.81	23.5	12.7	0.36	0.07	0.43	6.09	3.13	0.42	4.73	n.a.	9.05	691	0.076	8.83	1.55	12.9	0.20	0.090	127	n.a	0.044	n.a	3.13	1.24	0.20	0.27	n.a.	32.4	n.a.
11	Lower Agrio river (Salto del Agrio)	VH S	17/02/ 2017	0.45	13.7	8.58	0.065	0.05	0.13	1.19	0.025	0.25	0.95	n.a.	4.48	323	0.15	2.04	0.19	9.58	n.d.	0.052	85.4	n.a	n.d.	n.a	1.75	0.31	0.018	0.077	n.a.	6.40	n.a.
11	Lower Agrio river (Salto del Agrio)	VH S	26/02/ 2018	0.66	18.0	10.5	0.20	0.11	0.24	3.20	1.39	0.34	2.77	0.003	5.90	468	3.61	5.09	0.85	9.77	0.15	0.86	91.5	n.d.	0.022	0.020	2.05	0.76	0.13	0.17	4.67	29.6	0.022
12	Lower Agrio river (Puerta de Trolop e)	VH S	17/02/ 2017	0.44	33.7	14.1	0.10	0.06	0.14	1.19	0.047	0.32	1.15	n.a.	5.49	431	0.050	2.03	0.43	13.0	n.d.	0.088	111	n.a	0.008	n.a	2.43	0.47	0.021	0.069	n.a.	9.50	n.a.
13	Lower Agrio river (Before Ñorqui n river)	VH S	17/02/ 2017	0.48	13.6	8.73	0.028	0.05	0.070	0.27	0.049	0.20	1.27	n.a.	2.38	56.5	n.d.	0.47	0.15	13.5	n.a	0.057	178	n.a	0.009	n.a	3.90	0.19	0.020	1.80	n.a.	16.4	n.a.
14	Lower Agrio river (After Ñorqui n river)	VH S	17/02/ 2017	0.77	12.7	7.44	0.019	0.04	0.050	0.18	0.065	0.14	0.91	n.a.	1.92	36.3	0.15	0.39	0.24	10.2	0.072	0.15	148	n.a	n.d.	n.a	3.55	0.16	0.085	4.74	n.a.	4.56	n.a.
15	Pucón Mahui da stream	MW	12/02/ 2017	0.26	38.6	12.1	0.28	0.014	0.54	14.3	0.049	1.38	1.96	n.a.	1.8	201.5	0.26	22.9	0.10	20.6	0.47	0.13	219	n.a	0.009	n.a	3.89	0.14	0.16	0.19	n.a.	28.4	n.a.
15	Pucón Mahui da stream	MW	02/03/ 2018	0.43	37.0	12.7	0.18	n.d.	0.59	14.0	0.019	1.57	2.06	0.05	21.5	224.3	0.23	21.0	0.16	21.9	0.49	0.045	217	0.001	n.d.	n.d.	2.83	0.13	0.13	0.19	19.7	30.9	0.018
16	Trolop e river	MW	17/02/ 2017	0.33	7.98	3.24	n.d.	0.05	0.041	0.14	0.024	0.10	1.05	n.a.	2.67	66.5	0.25	1.58	0.16	4.98	n.d.	0.031	41.7	n.a	n.d.	n.a	1.12	0.035	0.010	0.32	n.a.	3.56	n.a.
17	Ñorqui n River	MW	17/02/ 2017	1.90	12.5	4.58	n.d.	0.04	0.030	0.15	0.020	0.012	0.81	n.a.	n.d.	27.3	0.47	0.20	0.10	3.81	0.07	139	n.a	n.d.	n.a	3.51	0.024	0.25	15.8	n.a.	1.29	n.a.	
19	Colora do stream	VH S	12/02/ 2017	0.87	43.5	12.9	4.88	0.014	3.76	19.6	0.47	4.23	5.89	n.a.	29.5	403.55	1.33	21.1	0.22	11.4	0.20	0.103	1203	n.a	0.058	n.a	6.21	0.50	0.38	0.36	n.a.	83.6	n.a.
19	Colora do stream	VH S	02/03/ 2018	1.07	16.9	11.5	2.01	n.d.	1.55	11.9	0.36	2.79	9.03	0.025	16.0	254.59	0.56	11.0	0.024	72.8	0.11	n.d.	716	0.007	0.024	0.034	4.43	0.38	0.60	0.11	71.9	10.8	0.073
20	Las Máqui nas	SH W	13/02/ 2017	1.37	39.54	42.9	0.39	0.023	5.66	1.09	4.53	0.77	0.34	n.a.	13.8	258	0.27	1.71	0.86	21.2	n.d.	0.038	178	n.a	0.016	n.a	12.6	0.10	0.16	17.9	n.a.	68.4	n.a.
20	Las Máqui nas	SH W	26/02/ 2018	1.77	39.25	44.7	0.27	0.012	0.10	2.59	3.78	0.73	2.20	n.d.	14.1	278	0.16	3.24	1.56	18.5	n.d.	n.d.	146	n.d.	n.d.	0.12	11.3	0.019	0.19	16.4	6.21	12.1	0.11
21	Las Maqui nitas	SH W	13/02/ 2017	2.07	53.2	16.1	1.24	0.034	3.95	0.46	4.32	2.35	0.59	n.a.	2.90	411	0.25	1.10	0.46	61.8	n.d.	0.078	67.1	n.a	n.d.	n.a	25.4	0.19	0.79	37.5	n.a.	92.4	n.a.
21	Las Maqui nitas	SH W	26/02/ 2018	10.9	45.7	39.6	3.28	0.069	0.34	7.50	25.1	5.36	6.04	0.041	15.9	182.5	0.14	8.80	2.07	13.4	n.d.	0.19	195	n.d.	n.d.	7.90	50.1	0.28	2.26	17.8	63.3	27.6	1.18
22	Agua del Limón	SH W	13/02/ 2017	2.98	n.d.	38.6	0.59	0.048	0.81	2.09	4.11	2.44	3.61	n.a.	2.24	526	1.05	3.18	5.45	72.7	0.30	0.091	93.4	n.a	n.d.	n.a	37.3	0.28	0.28	26.1	n.a.	37.0	n.a.
22	Agua del Limón	SH W	26/02/ 2018	2.77	8.99	31.1	0.43	0.04	n.d.	2.31	3.54	2.78	4.15	0.027	5.29	611	0.27	2.87	3.15	74.1	n.d.	0.044	59.3	n.a	n.d.	1.13	25.0	0.085	0.20	25.5	10.3	10.6	1.01
-	Averag e rock compo sition (Roulle	Roc k sam ple	-	7	-	476	2	-	-	26	78.7	2.82	52.5	4.58	-	0.136	3.25	35	13.6	58.6	-	2	517.5	0.6	-	8.01	1.23	0.2	2.3	17.9.8	26.1	83.7	20.4.7

Concentrations are in $\mu\text{g/L}$. n.a. is not analyzed, n.d. is not detected. VHS: Volcanic hydrological system; SHW: Steam

heated waters; MW: Melt waters. Rock concentrations are in mg/kg, Mn and Ti are in oxide weight %.

Table 3: REE concentrations in samples from 2018 campaign and an average rock composition

(Roulleau et al., 2018).

Sit e	Sample	Gro up	Date	La	Ce	Pr	Nd	S m	Eu	Gd	Tb	Dy	Ho	Er	Tm	Yb	Lu	La/S m	Gd/ Lu	Eu/E u*	Ce/C e*
1	Crater lake (cold lake)	MW	27/02/2018	1.64	3.95	0.51	2.16	0.47	0.1	0.45	0.1	0.34	0.1	0.19	0.1	0.15	0.1	0.61	2.09	0.75	1.10
2	South spring	VHS	27/02/2018	41.4	705	75.2	318	78.9	20.1	88.5	14.5	82.4	18.4	54.9	7.9	50.9	8.03	0.92	1.10	1.04	1.02
3	North spring	VHS	27/02/2018	36.6	591	60.0	25.0	58.0	14.0	60.2	9.2	51.8	11.2	32.5	4.65	29.8	4.63	1.11	1.29	1.03	1.02
5	Upper Agrio river (Ski station)	VHS	02/03/2018	33.0	577	61.8	26.5	63.5	15.2	68.7	10.9	61.5	13.5	39.7	5.72	36.6	5.71	0.91	1.20	1.00	1.03
8	Upper Agrio river (Bridge)	VHS	28/02/2018	75.8	133	15.5	66.5	15.6	3.50	16.7	2.62	14.6	3.21	9.19	1.32	8.35	1.30	0.85	1.28	0.94	0.99
9	Caviahu e lake	VHS	28/02/2018	7.02	15.1	1.93	8.21	1.71	0.35	1.77	0.26	1.40	0.30	0.85	0.11	0.73	0.11	0.72	1.53	0.88	1.04
11	Lower Agrio river (Salto del Agrio)	VHS	26/02/2018	4.11	6.66	1.03	4.19	0.86	0.15	0.87	0.13	0.73	0.15	0.44	0.1	0.37	0.1	0.83	1.51	0.76	0.82
15	Pucón Mahuida stream	MW	02/03/2018	13.0	24.6	3.45	14.6	2.77	0.42	3.19	0.46	2.46	0.53	1.41	0.17	0.84	0.13	0.82	2.44	0.62	0.94
19	Colorado stream	VHS	02/03/2018	27.1	78.5	9.64	43.2	9.26	1.49	11.0	1.68	9.40	2.11	5.97	0.80	4.74	0.75	0.51	1.45	0.64	1.20
20	Las Máquinas	SH W	26/02/2018	3.42	8.70	1.22	5.46	1.36	0.32	1.32	0.20	1.13	0.24	0.67	0.1	0.57	0.1	0.44	1.47	1.04	1.09
21	Las Maquinistas	SH W	26/02/2018	19.8	60.7	9.54	46.9	12.1	2.93	12.3	1.98	11.3	2.39	6.91	1.00	6.45	0.96	0.29	1.27	1.04	1.13
22	Agua del	SH W	26/02/2018	5.38	11.0	1.46	6.19	1.66	0.53	2.00	0.32	1.85	0.39	1.10	0.15	1.01	0.15	0.57	1.32	1.20	1.00

Journal Pre-proof																					
	Limón																				
1	Crater lake (Gamm ons et al. 2005)	VHS	15/03/1997	660	1400	180	720	150	34	150	22	110	22	64	9.5	63	9.0	0.77	1.65	0.98	1.09

Concentrations are in µg/L. n.a. is not analyzed. VHS: Volcanic hydrological system; SHW: Steam heated water; MW:

Melt waters. REE ratios are normalized by NASC (Gromet et al., 1984).

Declaration of interests

☒ The authors declare that they have no known competing financial interests or personal relationships that could have appeared to influence the work reported in this paper.

☐ The authors declare the following financial interests/personal relationships which may be considered as potential competing interests:

Highlights**“Hydrogeochemistry of trace and rare earth elements in the Cavihue-Copahue Volcanic Complex”**

1. Volatile elements as As, B, Cd, Se, Tl, and Te are supplied by magmatic gases
2. As, V, and Cr co-precipitate with Al and Fe when the pH increases.
3. Copahue volcano activity has increased from 2017 to 2018

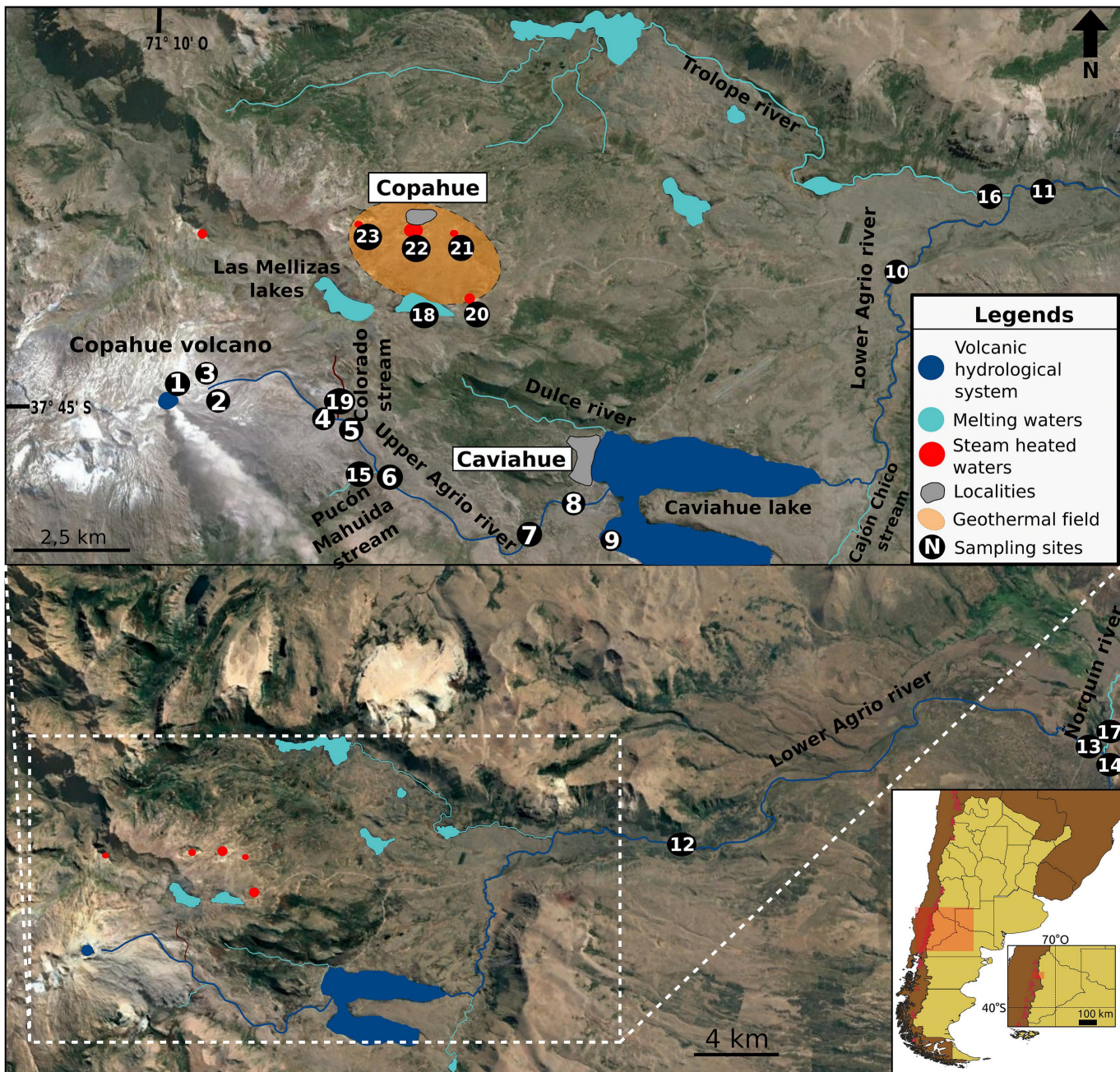


Figure 1



Figure 2

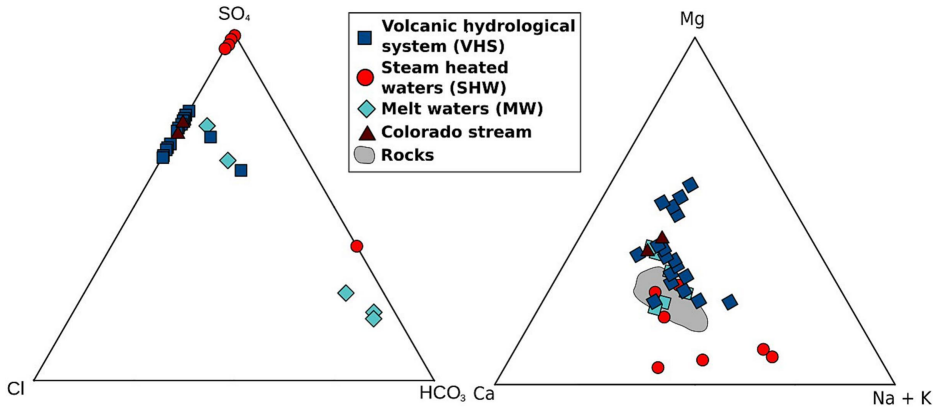


Figure 3

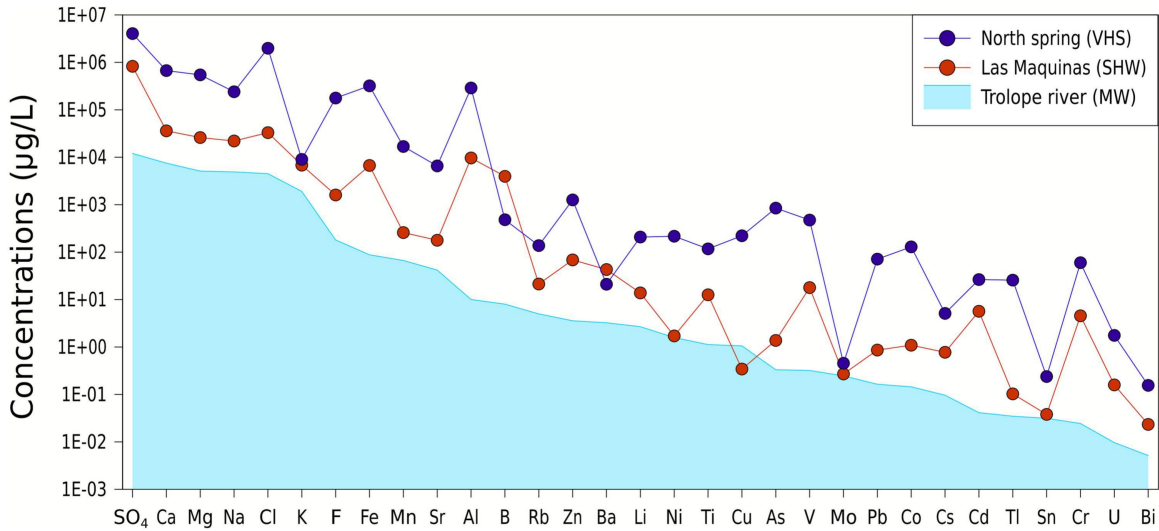


Figure 4

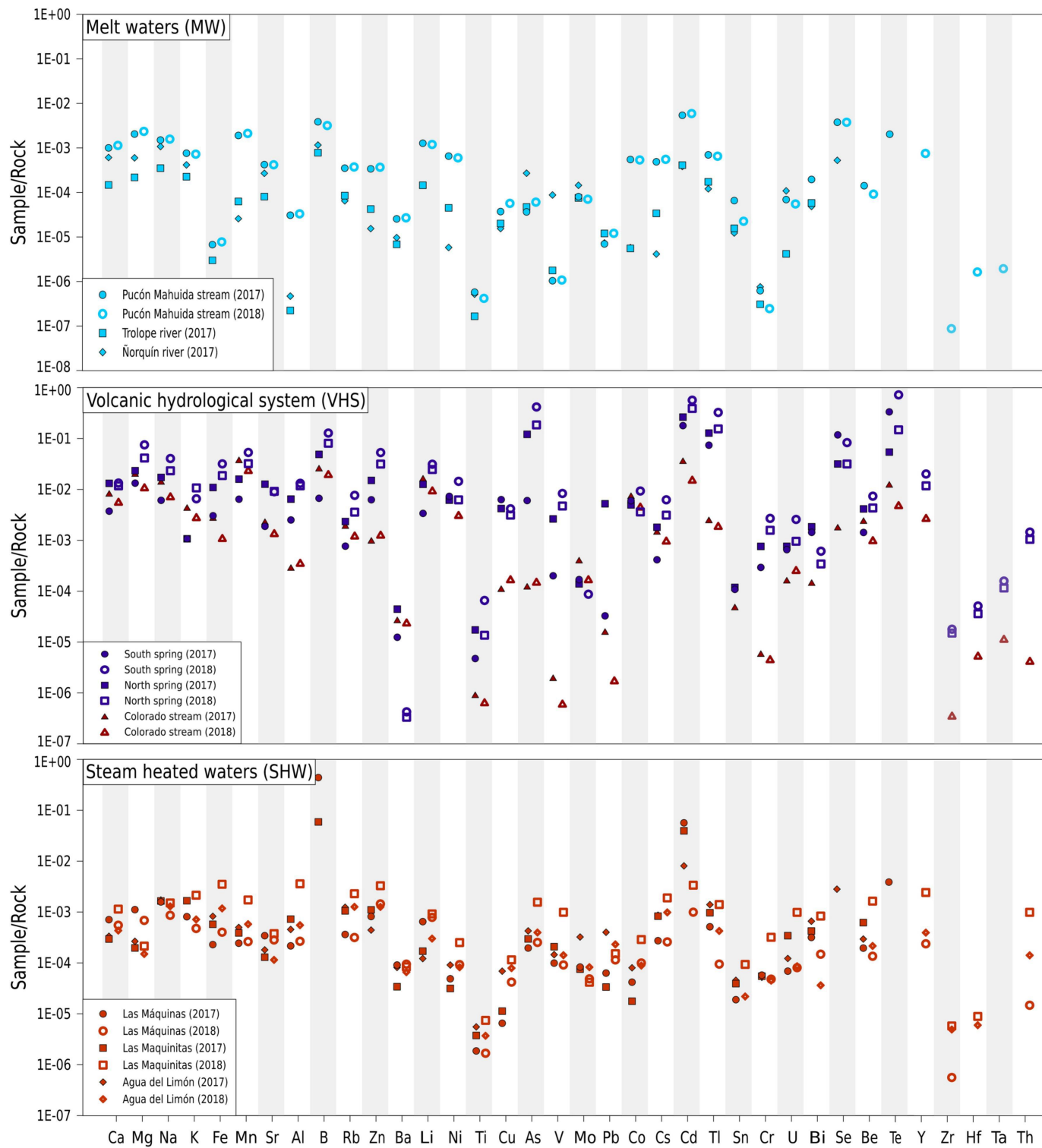


Figure 5

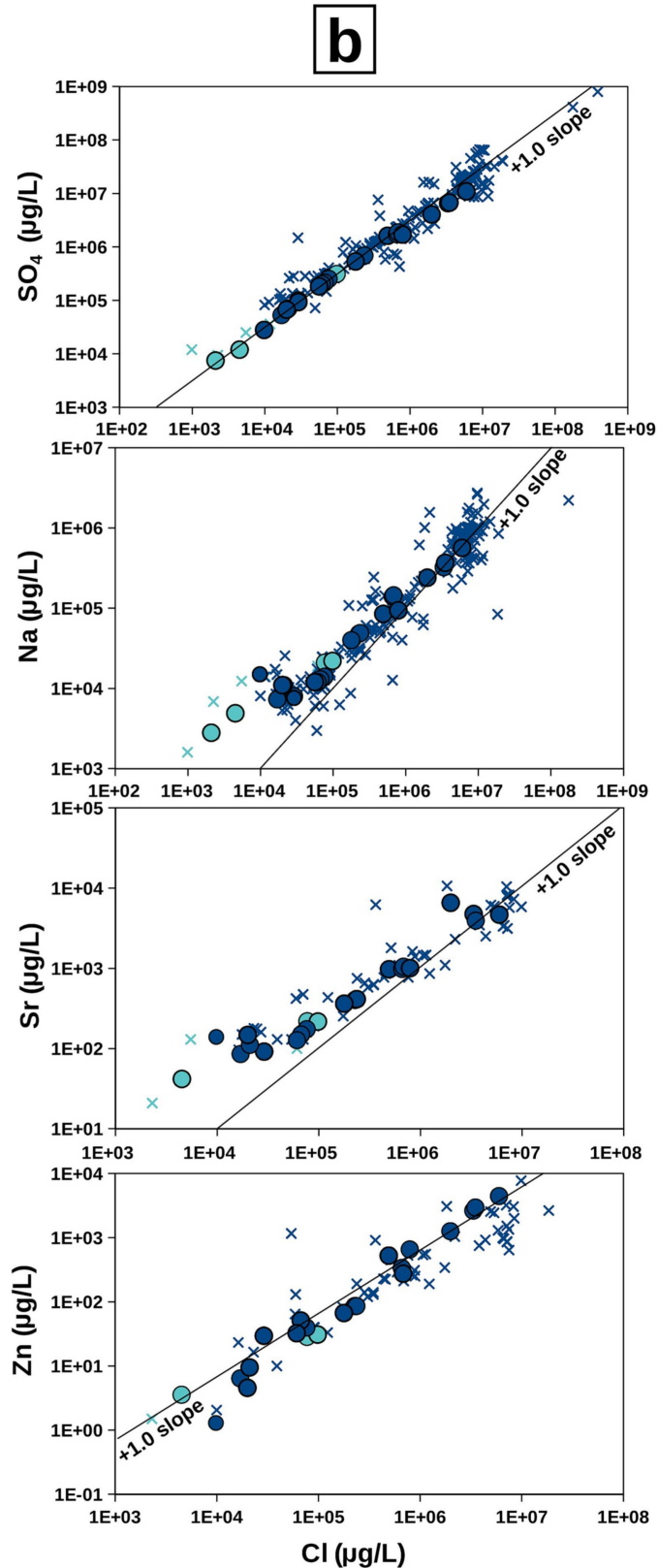
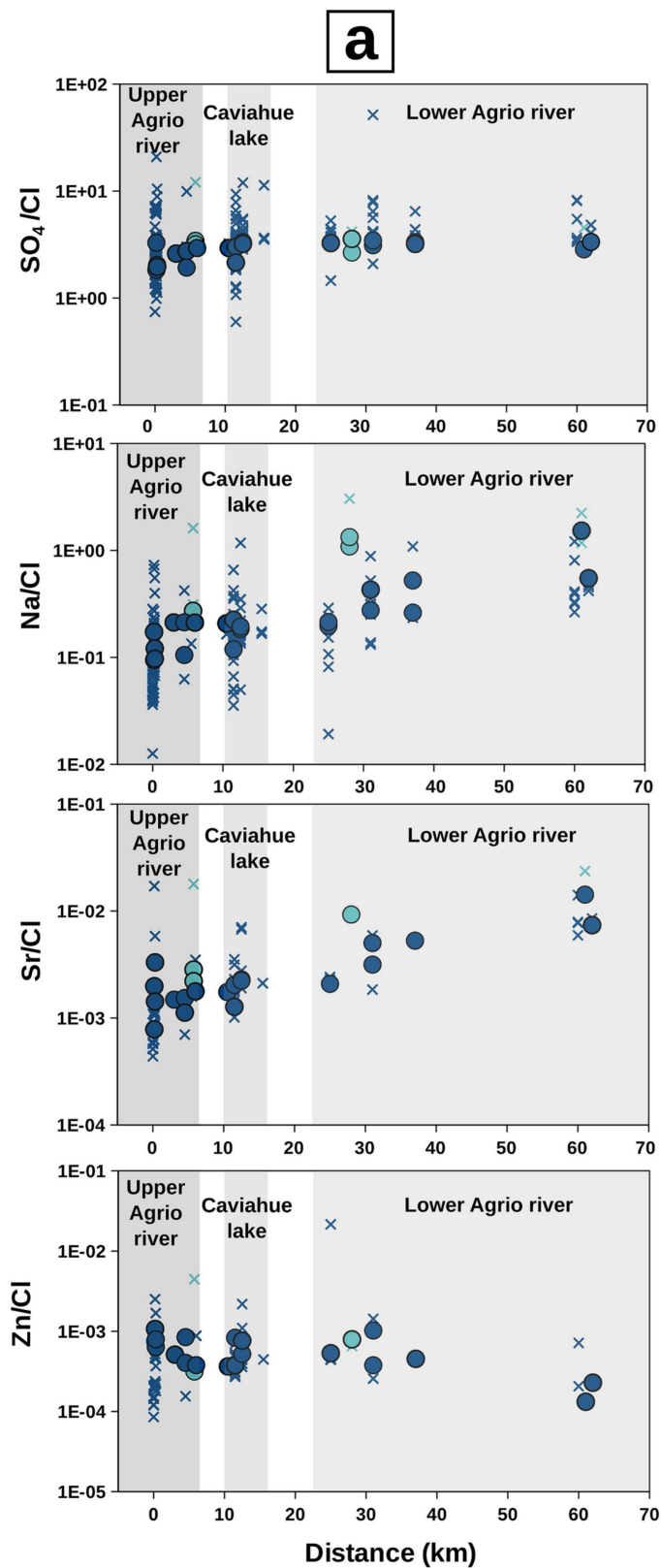


Figure 6

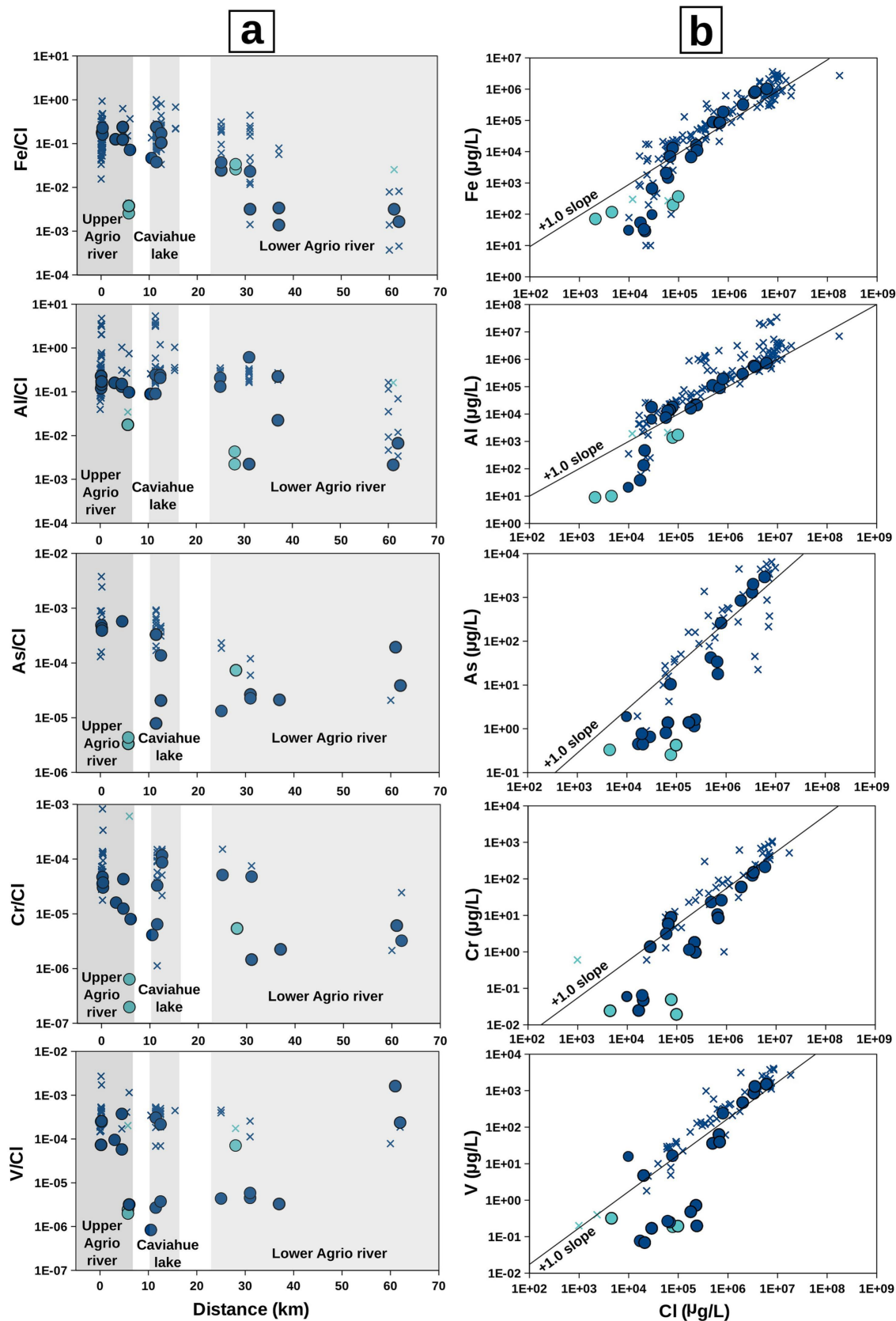


Figure 7

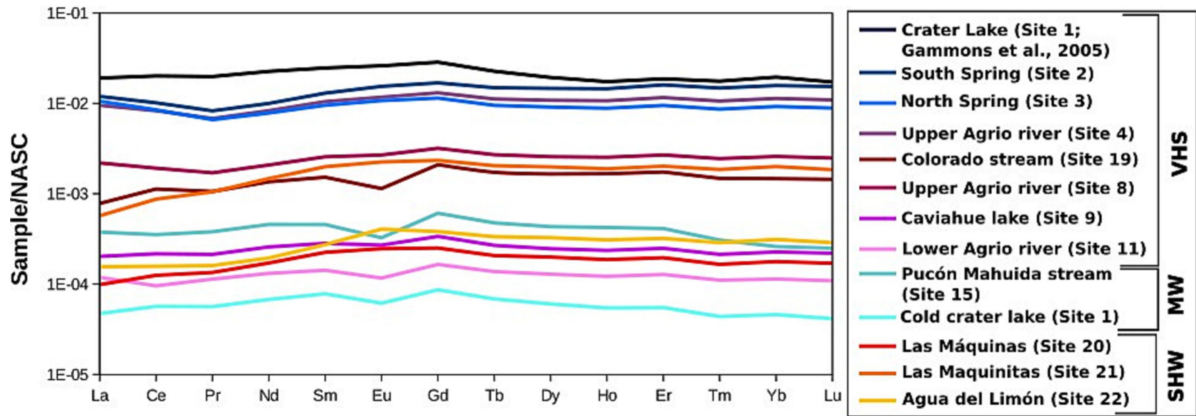


Figure 8

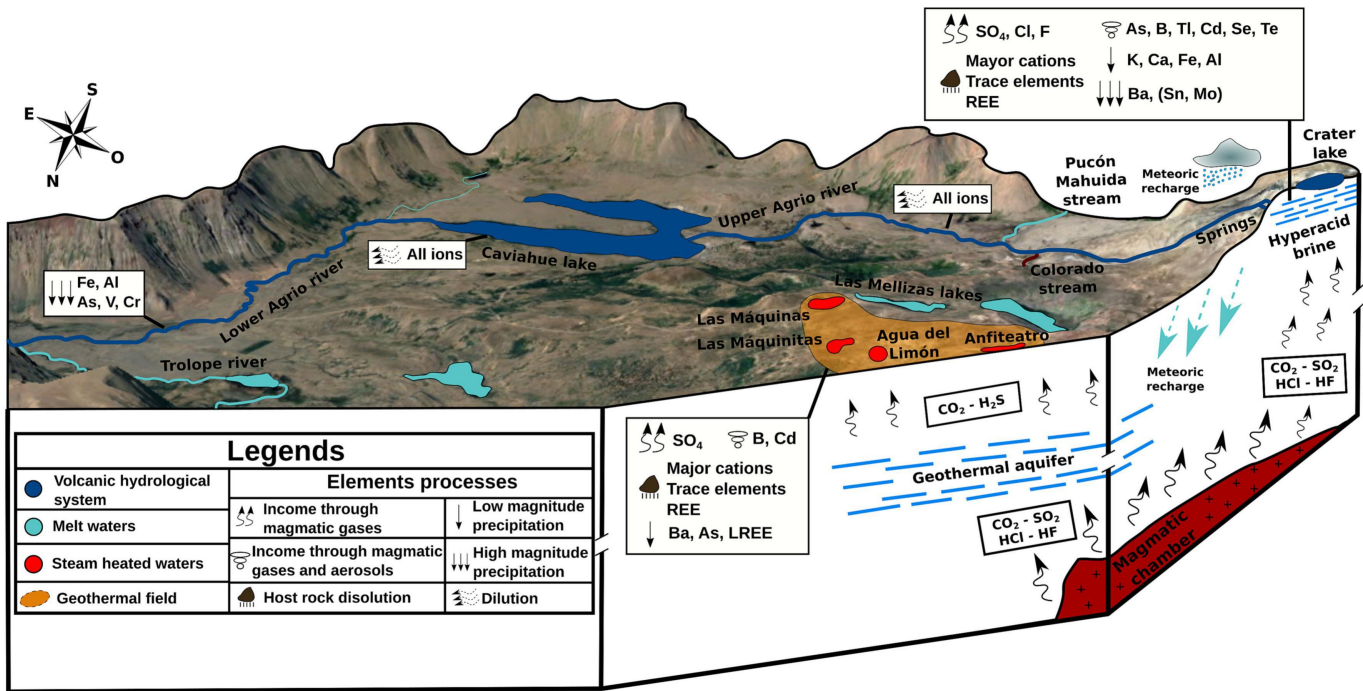


Figure 9